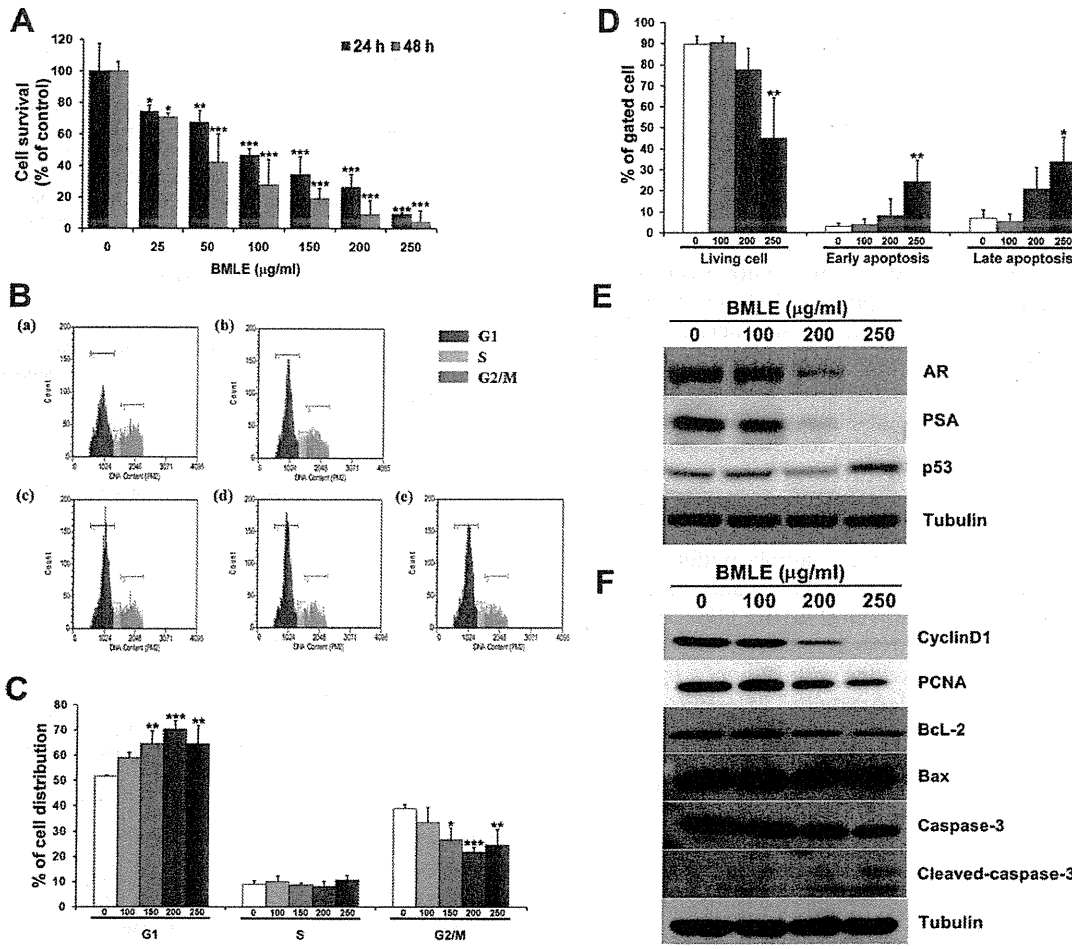

Fig. 1. BMLE caused G1 arrest and apoptosis induction in LNCaP cells. After incubation with 0–250 μg/ml BMLE for 24 and 48 h cytotoxicity was assessed by WST-1 assay (A). Histogram of cell cycle distribution (B) of LNCaP cells treated with vehicle control (a), 100 (b), 150 (c), 200 (d) and 250 (e) μg/ml BMLE for 48 h. Data analysis of cell cycle analyses (C) and apoptosis assays (D) of BMLE-treated LNCaP cells after 48 h of the treatment. The WST-1 results are expressed as percentages of vehicle control values. Data are mean ± SD values from three independent experiments. $^{*}P < 0.05$, $^{**}P < 0.01$ and $^{***}P < 0.001$, versus vehicle control. Immunoblot analysis of the protein levels of (E) AR, PSA, p53, (F) cell cycle-related proteins (cyclin D1 and PCNA) and apoptosis-related proteins (BcL-2, Bax, caspase-3 and cleaved-caspase-3) after treatment with vehicle control or BMLE for 48 h. The immunoblots shown here are representative of three independent experiments with similar results. Tubulin was employed as a loading control.

3.6. KuJ caused G1 cell cycle arrest in LNCaP cells

Based on the inhibitory effects of KuJ on LNCaP cell growth, the concentration of 15, 20, 25, and 30 μM of KuJ were selected for further *in vitro* mechanistic studies. As we found a significant effect of BMLE on cell cycle arrest in LNCaP, we thus determined the possible inhibitory effect of KuJ on cell cycle progression. As shown in Fig. 3A, treatment of LNCaP cells with KuJ for 24 and 48 h resulted in a significantly higher proportion of cells in the G1 phase at the concentrations used, 15 μM (67%, $p < 0.001$ and 64%, $p < 0.001$), 20 μM (70%, $p < 0.001$ and 69%, $p < 0.001$), 25 μM (64%, $p < 0.01$ and 63%, $p < 0.01$), and 30 μmol/L (59% and 64%, $p < 0.05$), compared with controls (55% and 53%). There was a concomitant reduction in the contributions of cells in the S and G2-M phases. These data suggest that inhibition of cell proliferation in LNCaP by KuJ might be associated with the induction of G1 arrest.

3.7. Induction of apoptosis by KuJ in LNCaP cells

To determine whether the KuJ-induced loss of the proliferation capacity and cell viability of LNCaP cells was associated with the induction of apoptosis, the cells were treated with KuJ as described above and the numbers of apoptotic cells were assessed. Apoptotic cells were counted as living cells and late or early apoptotic cells, which are presented in Fig. 3B. Treatment of KuJ for 24 h at 30 μM slightly but significantly induced apoptosis of LNCaP cells compare to controls (Fig. 3Ba). Treatment of LNCaP cells by 25 and 30 μM of KuJ for 48 h resulted in significant enhancement in the number of apoptotic cells in both the early and late stages of apoptosis (Fig. 3Bb): control (6% and 5%), 25 μM (33%, $P < 0.01$ and 15%, $P < 0.05$) and 30 μM (40%, $P < 0.01$ and 40%, $P < 0.001$).

3.8. Alteration of cell cycle- and apoptosis-related protein levels by KuJ

We next determined the expression of AR, PSA, and p53 and found that after 48 h treatment, KuJ reduced the protein expression of AR and PSA while enhancing the level of p53 in LNCaP cells in a concentration-dependent manner (Fig. 4A).

The expression of Cdk inhibitors, p21 and p27, which regulate the progression of cells in the G1 phase were assessed. Protein levels of p21 and p27 were increased following treatment with 15 and 20 μM KuJ for 48 h. On the other hand, the protein level of p21 was decreased, while the expression of p27 was still induced by treatment with 25 and 30 μM KuJ (Fig. 4B). Additionally, the expression of G1 positive regulators (cyclin D1, cyclin E, Cdk2, Cdk4 and PCNA) was down-regulated in a concentration-dependent manner (Fig. 4B).

We next determine whether the protein levels of apoptosis-involving proteins would be altered by KuJ. Treatment with KuJ at 15 and 20 μM resulted in a concentration-dependent reduction in the levels of the anti-apoptotic protein Bcl-xL with a concomitant increase in the level of pro-apoptotic protein Bad, while that of Bax was not changed (Fig. 4C). KuJ treatment at 25 and 30 μM dramatically decreased the protein

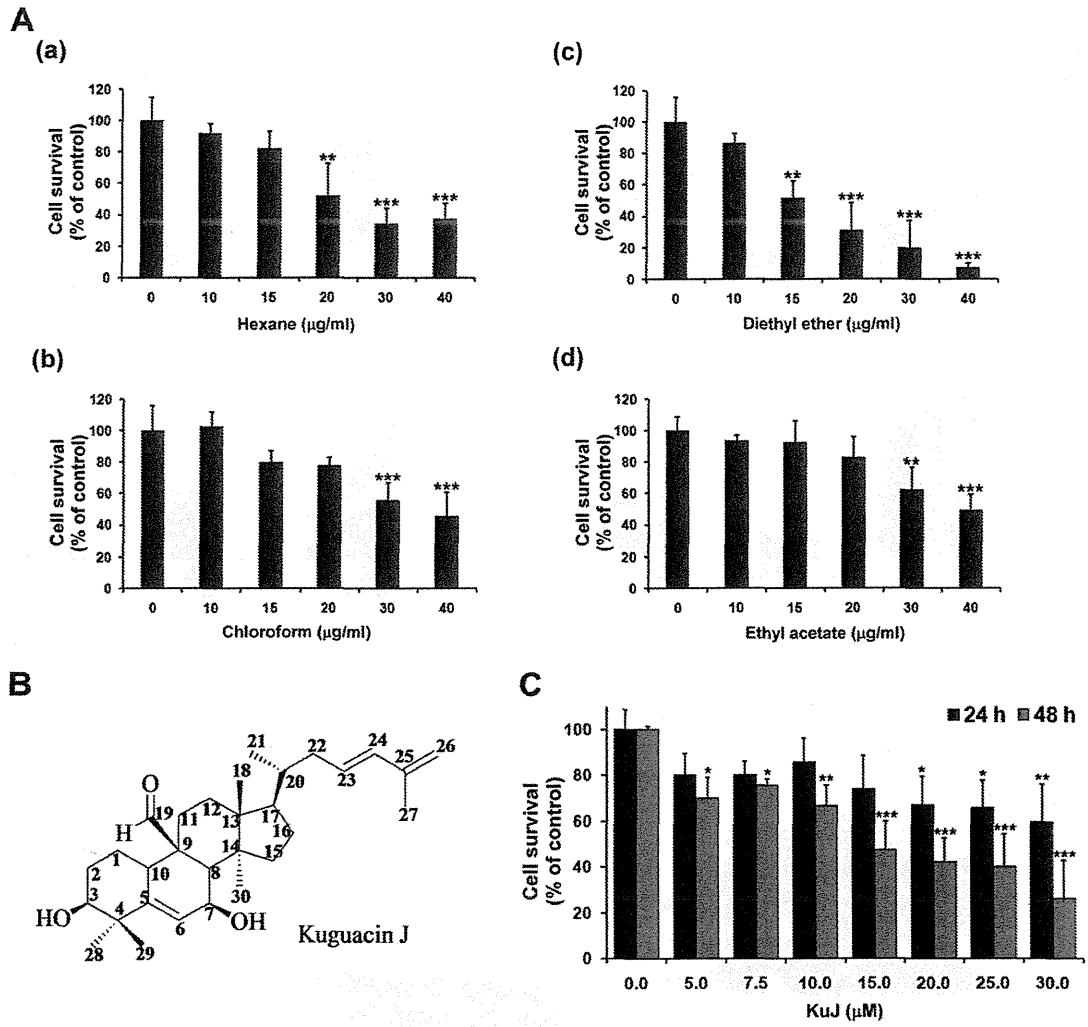

Fig. 2. Characterization of an active component in BMLE. (A) Cells were treated with 0–40 μg/ml of organic fractions obtained by partition–extraction using: (a) hexane, (b) diethyl ether, (c) chloroform and (d) ethyl acetate for 48 h and then WST-1 assays were perform to determine their growth inhibitory effects. (B) Structural formula of KuJ. (C) KuJ showed growth suppression in LNCaP cells as demonstrated by the WST-1 assay. The results are expressed as percentages of the vehicle control group value. Data are mean ± SD values from three independent experiments. $^{*}P < 0.05$, $^{**}P < 0.01$ and $^{***}P < 0.001$, versus control.

expression of Bcl-xL and Bcl-2 and slightly reduced the level of Bad and Bax. Band density analyses indicated that while KuJ treatment caused an overall decrease in expression of pro-apoptotic proteins, at the same time it elevated the ratios of Bax/Bcl-2 and Bad/Bcl-xL, which could initiate the caspase activation pathway for apoptosis (Data not shown) Likewise, KuJ treatment at dose of 25 and 30 μM, dramatically decreased the expression of survivin and caspase-3 and increased the expression of cleaved caspase-3 accompanied by cleavage of PARP.

The results demonstrated that KuJ altered the expressions of cell cycle- and apoptosis-regulatory proteins contributed to G1 arrest and apoptosis induction in LNCaP cells.

3.9. p53-dependent cell cycle arrest and apoptosis induction by KuJ in LNCaP cells

The induction of p53 might be a one possibility for BMLE and KuJ to trigger LNCaP cell growth. To investigate this mechanism, the cells were transfected with p53 siRNA follow by BMLE or KuJ treatment. The efficiency of p53 siRNA was proven with reference to decrease of p53 protein expression using western blotting analysis, and the expression of p21, a downstream target of p53 also was determined (Fig. 5A). In LNCaP cells, p53 protein expression was knocked down by treatment of p53 siRNA for 24 h compared with the control siRNA. Then the cells were treated with BMLE (250 μg/ml) or KuJ (25 μM) and the percentage cell distribution and apoptotic cell death were determined. As shown in Fig. 5B and C, transfection of p53 siRNA in LNCaP cells significantly reversed BMLE-induced cell cycle arrest, but slightly decreased KuJ-induced arrest of the cell cycle. Furthermore, the increase of the number of apoptotic cells by BMLE and KuJ was dramatically reduced when the cells were pre-treated with p53 siRNA (Fig. 5D and E).

3.10. Cytotoxicity of BMLE and KuJ in PNT1A cells

PNT1A cells were treated with various concentrations of BMLE or KuJ for 24 h and 48 h, and cell viability were assessed by WST-1 assay. With BMLE treatment, the viability of the cells was significantly reduced at concentrations between 200 and 250 μg/ml. The IC 50 values for BMLE were approximately 100 μg/ml and 50 μg/ml for 24 h and 48 h treatment, respectively (Fig. 6A). Cell viability was significantly decreased by KuJ at concentrations between 25 and 30 μM for 24 h and 20–30 μM for 48 h treatment. The IC 50 was more than 30 μM for both 24 h and 48 h treatment, (Fig. 6B). In contrast to the effect of BMLE and KuJ in cancer cell line, LNCaP, the results showed that the both compounds caused less toxicity in non-neoplastic human prostate epithelial cells.

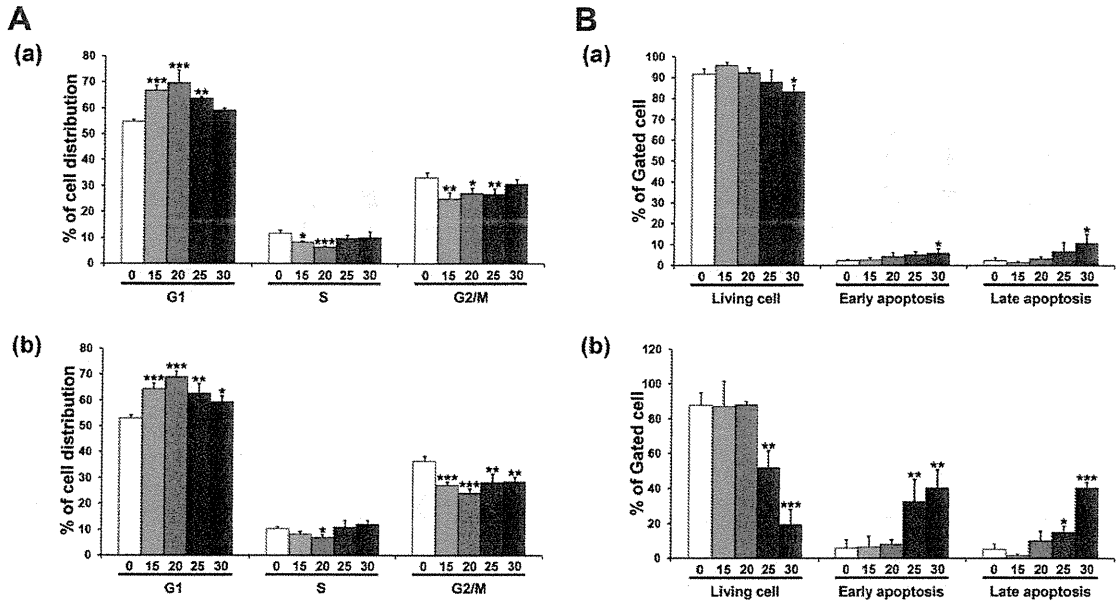

Fig. 3. Effects of KuJ on cell cycle progression and apoptosis induction in LNCaP cells. After treatment with 0, 15, 20, 25 and 30 μM KuJ, cells were harvested for analysis of cell cycle distribution and apoptosis. (A) LNCaP cell cycle distribution after treatment with KuJ for 24 (a) and 48 h (b). (B) Percentage of living cells, early and late apoptoses were summarized after 24 (a) and 48 h (b) of KuJ treatment. Data are mean ± SD values from three independent experiments. $^{*}P < 0.05$, $^{**}P < 0.01$ and $^{***}P < 0.001$, versus vehicle control.

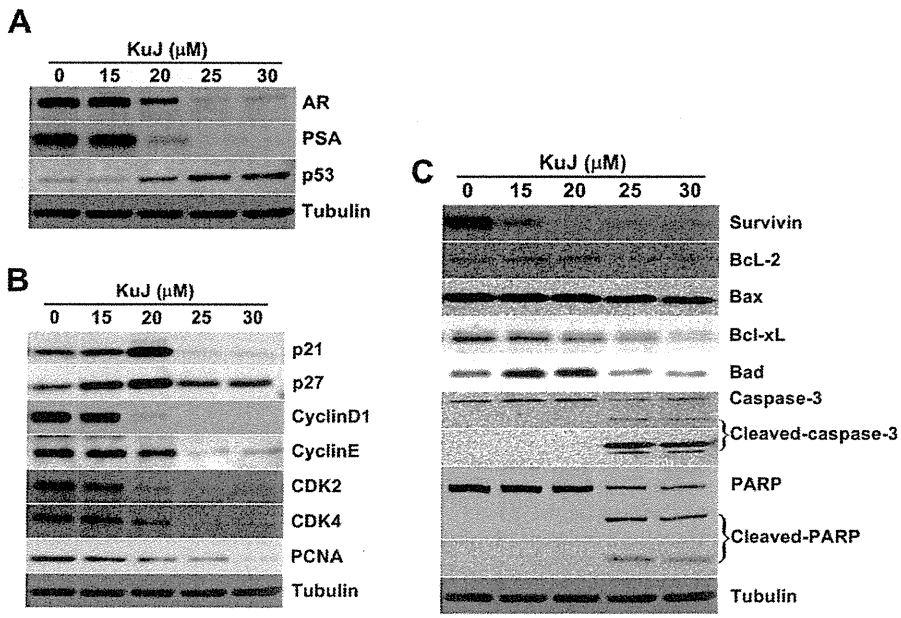

Fig. 4. KuJ alteration of the expression of cell cycle- and apoptosis-involving proteins. Immunoblot analysis of the protein levels of AR, PSA, p53 (A), cell cycle-related proteins (p21, p27, cyclin D1, cyclinE, CDK2, CDK4 and PCNA); (B) and apoptosis-related proteins (survivin, BcL-2, Bax, Bcl-xL, Bad, caspase-3, cleaved-caspase-3, PARP and cleaved-PARP); (C) after treatment with vehicle control or KuJ for 48 h. The immunoblots shown here are representative of three independent experiments with similar results. Tubulin was employed as a loading control.

4. Discussion

Fruits, vegetables, and common beverages, as well as several herbs and plants with diversified pharmacological properties, have been shown to be rich sources of micro-chemicals with the potential to prevent human cancers [29,30]. Prostate cancer is an ideal disease for chemopreventive intervention as it grows slowly before the onset of symptoms and the establishment of diagnosis, which usually occurs in men more than 50 years of age. Therefore, pharmacological or nutritional intervention could considerably impact the quality of life of patients by delaying the progression of cancer [5]. The present study found that BMLE exerted significant growth inhibitory

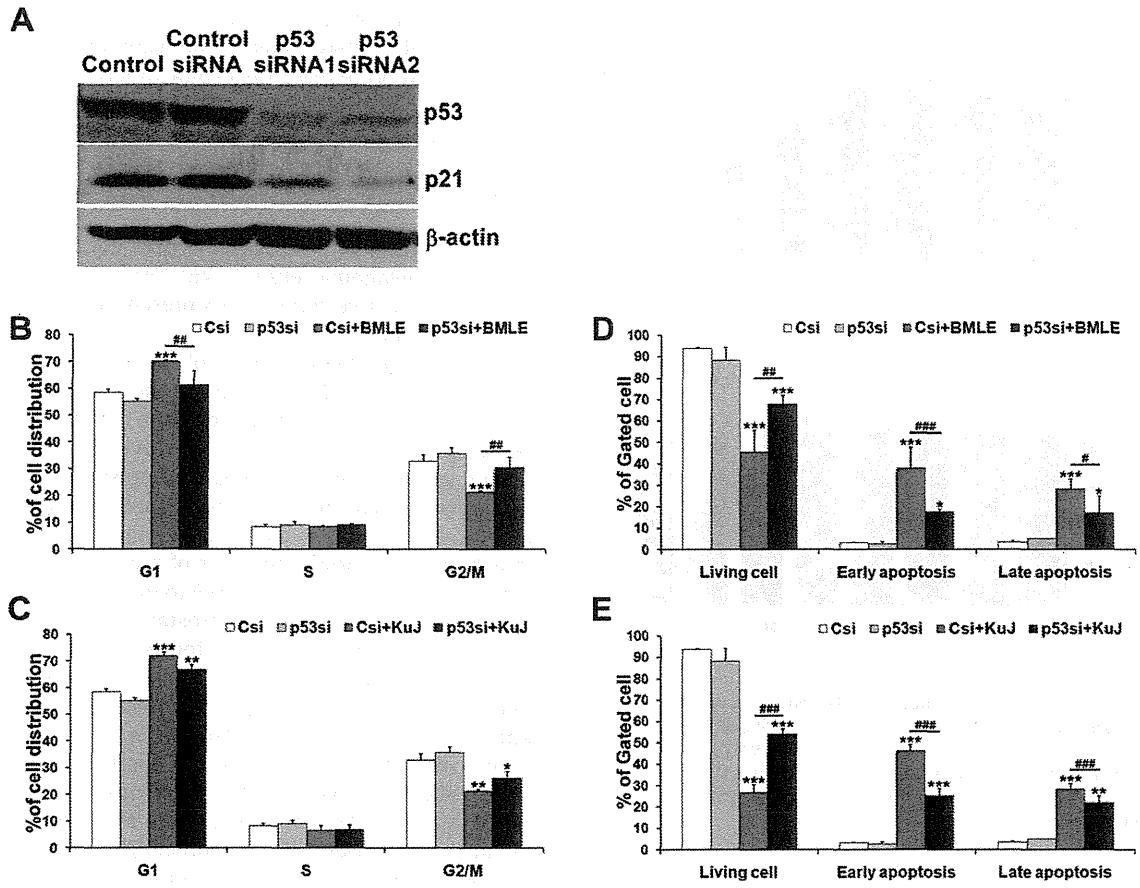

Fig. 5. BMLE and KuJ induction of p53-mediated cell cycle arrest and apoptosis in LNCaP. (A) Efficiency of p53 knockdown by 20 nM p53 siRNA was verified using Western blotting at 24 h post transfection. Cell cycle distribution and apoptosis were estimated when siRNA-transfected LNCaP cells were treated with (B and D) 250 μg/ml BMLE and (C and E) 25 μM KuJ. Data are mean ± SD values from three independent experiments. * or $^{\#}P < 0.05$, ** or $^{\#\#}P < 0.01$ and *** or $^{\#\#\#}P < 0.001$, versus control.

effects on LNCaP cells via induction of G1 arrest and apoptosis cell death. Thus identification of anti-cancer component(s) in BMLE could be valuable for prevention and intervention of cancers and the partition–extraction yielded four organic fractions, among which, DEF exerted the highest growth inhibitory effects. After the isolation using DEF as a starting material, KuJ, a known triterpenoid was obtained which also caused dramatic decrease of LNCaP cell proliferation and viability, indicating that it is at least one active component in BMLE.

Regulation of cell cycle progression in cancer cells is considered to be a potentially effective mechanism for control of tumor growth [31,32]. Molecular analyses of human cancers have revealed that cell cycle regulators frequently often display abnormalities in encoding genes in most common malignancies [33,34]. Here, treatment of androgen-sensitive (LNCaP) cells with KuJ resulted in significant G1-phase arrest of cell cycle progression, along with reduction of cyclin D1, cyclinE, Cdk2 and Cdk4 and increase of p21 and p27 at the protein level. This indicates the KuJ-induced G1 arrest might be mediated through the up-regulation of p21 and p27 proteins, which enhance the formation of heterotrimeric complexes with G1-S Cdks and cyclins, thereby inhibiting their activity. Additionally, KuJ also dramatically suppressed the expression of a proliferation marker, PCNA, that is expressed in late G1 phase and early S phase [35]. The inhibition of cell proliferation or the induction of cell death in LNCaP by KuJ might be associated with G1 arrest machinery.

G1-phase arrest of cell cycle progression provides an opportunity for cells to either undergo repair or follow the apoptotic pathway, which plays a crucial role in tissue homeostatic eliminating mutated hyperproliferating neoplastic cells from the system. Acquired resistance toward apoptosis is a hallmark of most and perhaps all types of cancer. Therefore induction of apoptosis is considered to be one of protective mechanisms against cancer progression. In the present study, treatment of LNCaP cells with 25 and 30 μM of KuJ resulted in significant induction of apoptosis. Survivin is a member of the inhibitor of apoptosis protein family, involved in inhibition of apoptosis, exerts multiple effects throughout the cell cycle [36]. Our study revealed that KuJ treatment reduced the protein level of survivin, which might be associated with KuJ-induced cell cycle arrest and apoptosis in LNCaP cells. In addition, since the ratios of pro-apoptotic proteins (e.g., Bad and Bax) and anti-apoptotic proteins (e.g., Bcl-2 and Bcl-xL) are essential for the regulation of apoptosis through

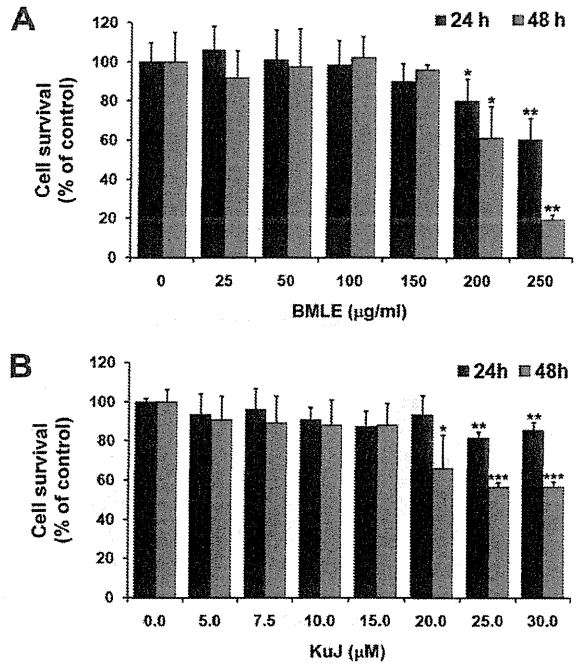

Fig. 6. Cytotoxicity of BMLE and KuJ in PNT1A cells. Cells were incubated with (A) 0–250 μg/ml BMLE or (B) 0–30 μM KuJ for 24 and 48 h and then cytotoxicity was assessed by WST-1 assay. The WST-1 results are percentages of vehicle control values. Data are mean ± SD values from three independent experiments. $^{*}P < 0.05$, $^{**}P < 0.01$ and $^{***}P < 0.001$, versus control.

caspase signaling [37], the finding that KuJ could alter the protein levels of key members of the Bcl-2 family in a manner that favors an increase in the ratios of Bax/Bcl-2 and Bad/Bcl-xLis of obvious significance.

AR is known to play a critical role in the development and progression of prostate cancer through alteration of the normal androgen axis by dysregulation of AR activity [38]. An ability of AR to cross-talk with several growth factor signaling cascades active regulation of cell cycle, apoptosis, and differentiation outcomes in prostate cancer cells has been reported [39]. The fact that KuJ decreased the expression of AR followed by reduction of protein level of PSA might be involved in KuJ-caused growth inhibition of LNCaP through the induction of G1 arrest and apoptosis.

The tumor suppressor p53 protein is a regulator of genotoxic stress that plays an important role in DNA damage response, DNA repair, cell cycle regulation, and in triggering apoptosis after cell injury [40]. Induction of apoptosis is considered to be a central to the tumor-suppressive function of p53 [41]. Knockdown of p53 by RNA interference in LNCaP slightly suppressed cell cycle arrest whereas it markedly abolished apoptosis induction by KuJ. These results indicate that KuJ induced p53-mediated partly cell cycle arrest and mainly apoptosis, which led to the inhibition of cell growth, and may be related with the activation of p53 signaling pathways.

Because KuJ was purified from BMLE, the two were compared. The growth inhibition effects of KuJ on LNCaP cells proved similar to those of BMLE. However, KuJ accounts for only approximately 1.6% of BMLE, and the effective concentration of KuJ was only 10-fold lower. Therefore, BMLE may include other compounds which also exert anti-tumor effects. Cucurbitacin B (cucB), a triterpenoid from Cucurbitaceae vegetables also found in bitter melon seeds, caused cell cycle arrest and apoptosis induction in human colon adenocarcinoma cancer cells [42]. Additionally, Rutin, a flavonoid present in bitter melon leaves, has been reported to show growth inhibition of leukemia and ovarian carcinoma cells, with anti-invasive effects on melanoma cells [43–46]. Therefore characterization of other active components present in BMLE has to be further explored.

Interestingly, the sensitivity of the human normal prostatic epithelial cell line, PNT1A, to the cytotoxic effects of BMLE and KuJ was much lower than that of LNCaP cells, pointing to potential use as effective chemopreventive agents against androgen-sensitive prostate cancer cells. In Asia people consume fruit and/or leaves of bitter melon as food [6,7] and this and other components of the diet may be linked to low incidences of prostate cancer in general [47].We have reported BMLE to inhibit the progression of androgen-independent rat prostate cancers *in vitro* and *in vivo* [19]. To provide a basis for use of KuJ as a broader antineoplastic agent for prostate cancer, further study is needed to investigate anti-cancer effects of KuJ on human androgen-independent prostate cancer.

In conclusion, we here report for the first time the ability of BMLE and KuJ to inhibit cell proliferation and viability through induction of G1-phase arrest and apoptosis on an androgen-dependent human prostate cancer cell line, while exhibiting only low toxicity in normal human prostate epithelial cells. In addition, we provide mechanistic evidence that KuJ-induced G1 arrest and apoptosis in prostate carcinoma cells might be partly mediated through enhanced expression of p53. Taking the results together, KuJ might be a promising candidate new chemopreventive agent for androgen-dependent prostate cancer.

Conflicts of interest

None declared.

Acknowledgment

This work was supported by grants from the Royal Golden Jubilee Ph.D. Program of Thailand, National Research Council of Thailand and the Society for Promotion of Pathology of Nagoya, Japan.

References

[1] H. Gronberg, Prostate cancer epidemiology, Lancet 361 (2003) 859–864.
[2] E. Bidoli, R. Talamini, C. Bosetti, E. Negri, D. Maruzzi, M. Montella, S. Franceschi, C. La Vecchia, Macronutrients, fatty acids, cholesterol and prostate cancer risk, Ann. Oncol. 16 (2005) 152–157.
[3] G.J. Kelloff, J.A. Crowell, V.E. Steele, R.A. Lubet, C.W. Boone, W.A. Malone, E.T. Hawk, R. Lieberman, J.A. Lawrence, L. Kopelovich, I. Ali, J.L. Viner, C.C. Sigman, Progress in cancer chemoprevention, Ann. N. Y. Acad. Sci. 889 (1999) 1–13.
[4] Y.J. Surh, Cancer chemoprevention with dietary phytochemicals, Nat. Rev. Cancer 3 (2003) 768–780.

[5] D.N. Syed, N. Khan, F. Afaq, H. Mukhtar, Chemoprevention of prostate cancer through dietary agents: progress and promise, Cancer Epidemiol. Biomarkers Prev. 16 (2007) 2193–2203.
[6] E. Basch, S. Gabardi, C. Ulbricht, Bitter melon (*Momordica charantia*): a review of efficacy and safety, Am. J. Health Syst. Pharm. 60 (2003) 356–359.
[7] A. Gurib-Fakim, A.H. Subratty, F. Mahomoodally, Bitter melon: an exotic vegetable with medicinal values, Nutr. Food Sci. 35 (2005) 143–147.
[8] F. Licastro, C. Franceschi, L. Barbieri, F. Stirpe, Toxicity of *Momordica charantia* lectin and inhibitor for human normal and leukaemic lymphocytes, Virchows Arch. B Cell Pathol. Incl. Mol. Pathol. 33 (1980) 257–265.
[9] T.B. Ng, W.K. Liu, S.F. Sze, H.W. Yeung, Action of alpha-momorcharin, a ribosome inactivating protein, on cultured tumor cell lines, Gen. Pharmacol. 25 (1994) 75–77.
[10] M.G. Battelli, L. Polito, A. Bolognesi, L. Lafleur, Y. Fradet, F. Stirpe, Toxicity of ribosome-inactivating proteins-containing immunotoxins to a human bladder carcinoma cell line, Int. J. Cancer 65 (1996) 485–490.
[11] C. Ganguly, S. De, S. Das, Prevention of carcinogen-induced mouse skin papilloma by whole fruit aqueous extract of *Momordica charantia*, Eur. J. Cancer Prev. 9 (2000) 283–288.
[12] Y. Sun, P.L. Huang, J.J. Li, Y.Q. Huang, L. Zhang, S. Lee-Huang, Anti-HIV agent MAP30 modulates the expression profile of viral and cellular genes for proliferation and apoptosis in AIDS-related lymphoma cells infected with Kaposi's sarcoma-associated virus, Biochem. Biophys. Res. Commun. 287 (2001) 983–994.
[13] H. Shi, M. Hiramatsu, M. Komatsu, T. Kayama, Antioxidant property of Fructus Momordicae extract, Biochem. Mol. Biol. Int. 40 (1996) 1111–1121.
[14] S. Lee-Huang, P.L. Huang, H.C. Chen, A. Bourinbaiar, H.I. Huang, H.F. Kung, Anti-HIV and anti-tumor activities of recombinant MAP30 from bitter melon, Gene 161 (1995) 151–156.
[15] M.J. Tan, J.M. Ye, N. Turner, C. Hohnen-Behrens, C.Q. Ke, C.P. Tang, T. Chen, H.C. Weiss, E.R. Gesing, A. Rowland, D.E. James, Y. Ye, Antidiabetic activities of triterpenoids isolated from bitter melon associated with activation of the AMPK pathway, Chem. Biol. 15 (2008) 263–273.
[16] J.E. Cunnick, K. Sakamoto, S.K. Chapes, G.W. Fortner, D.J. Takemoto, Induction of tumor cytotoxic immune cells using a protein from the bitter melon (*Momordica charantia*), Cell. Immunol. 126 (1990) 278–289.
[17] W.R. Kusamran, A. Ratanavila, A. Tepsuwan, Effects of neem flowers, Thai and Chinese bitter gourd fruits and sweet basil leaves on hepatic monooxygenases and glutathione S-transferase activities, and in vitro metabolic activation of chemical carcinogens in rats, Food Chem. Toxicol. 36 (1998) 475–484.
[18] P. Limtrakul, O. Khantamat, K. Pintha, Inhibition of P-glycoprotein activity and reversal of cancer multidrug resistance by *Momordica charantia* extract, Cancer Chemother. Pharmacol. 54 (2004) 525–530.
[19] P. Pitchakarn, K. Ogawa, S. Suzuki, S. Takahashi, M. Asamoto, T. Chewonarin, P. Limtrakul, T. Shirai, *Momordica charantia* leaf extract suppresses rat prostate cancer progression in vitro and in vivo, Cancer Sci. 101 (2010) 2234–2240.
[20] R.B. Ray, A. Raychoudhuri, R. Steele, P. Nerurkar, Bitter melon (*Momordica charantia*) extract inhibits breast cancer cell proliferation by modulating cell cycle regulatory genes and promotes apoptosis, Cancer Res. 70 (2010) 1925–1931.
[21] P. Pitchakarn, S. Ohnuma, K. Pintha, W. Pompimon, S. Ambudkar, P. Limtrakul, Kuguacin J isolated from *Momordica charantia* leaves inhibits P-glycoprotein (ABCB1)-mediated multidrug resistance, J. Nutr. Biochem., in press, doi:10.1016/j.jnutbio.2010.11.005.
[22] J. Chen, R. Tian, M. Qiu, L. Lu, Y. Zheng, Z. Zhang, Trinorcucurbitane and cucurbitane triterpenoids from the roots of *Momordica charantia*, Phytochemistry 69 (2008) 1043–1048.
[23] J.C. Chen, W.Q. Liu, L. Lu, M.H. Qiu, Y.T. Zheng, L.M. Yang, X.M. Zhang, L. Zhou, Z.R. Li, Kuguacins F-S, cucurbitane triterpenoids from *Momordica charantia*, Phytochemistry 70 (2009) 133–140.
[24] D.B. Mekuria, T. Kashiwagi, S. Tebayashi, C.S. Kim, Cucurbitane triterpenoid oviposition deterrent from *Momordica charantia* to the leafminer, *Liriomyza trifolii*, Biosci. Biotechnol. Biochem. 69 (2005) 1706–1710.
[25] N. Puspawati, Isolation and identification momordicin I from leaves extract of *Momordica charantia* L., J. KIMIA 2 (2008) 53–56.
[26] K. Hamasaki, K. Kogure, K. Ohwada, A biological method for the quantitative measurement of tetrodotoxin (TTX): tissue culture bioassay in combination with a water-soluble tetrazolium salt, Toxicon 34 (1996) 490–495.
[27] J.S. Horoszewicz, S.S. Leong, E. Kawinski, J.P. Karr, H. Rosenthal, T.M. Chu, E.A. Mirand, G.P. Murphy, LNCaP model of human prostatic carcinoma, Cancer Res. 43 (1983) 1809–1818.
[28] M. Burchardt, T. Burchardt, A. Shabsigh, M. Ghafar, M.W. Chen, A. Anastasiadis, A. de la Taille, A. Kiss, R. Buttyan, Reduction of wild type p53 function confers a hormone resistant phenotype on LNCaP prostate cancer cells, Prostate 48 (2001) 225–230.
[29] R.L. Thangapazham, A. Sharma, R.K. Maheshwari, Multiple molecular targets in cancer chemoprevention by curcumin, AAPS J. 8 (2006) E443–E449.
[30] N. Khan, V.M. Adhami, H. Mukhtar, Apoptosis by dietary agents for prevention and treatment of prostate cancer, Endocr. Relat. Cancer 17 (2010) R39–52.
[31] N.P. Pavletich, Mechanisms of cyclin-dependent kinase regulation: structures of Cdks, their cyclin activators, and Cip and INK4 inhibitors, J. Mol. Biol. 287 (1999) 821–828.
[32] R. Agarwal, Cell signaling and regulators of cell cycle as molecular targets for prostate cancer prevention by dietary agents, Biochem. Pharmacol. 60 (2000) 1051–1059.
[33] M. Nakanishi, M. Shimada, H. Niida, Genetic instability in cancer cells by impaired cell cycle checkpoints, Cancer Sci. 97 (2006) 984–989.
[34] W.K. Kaufmann, K.R. Nevis, P. Qu, J.G. Ibrahim, T. Zhou, Y. Zhou, D.A. Simpson, J. Helms-Deaton, M. Cordeiro-Stone, D.T. Moore, N.E. Thomas, H. Hao, Z. Liu, J.M. Shields, G.A. Scott, N.E. Sharpless, Defective cell cycle checkpoint functions in melanoma are associated with altered patterns of gene expression, J. Invest. Dermatol. 128 (2008) 175–187.
[35] G.L. Moldovan, B. Pfander, S. Jentsch, PCNA, the maestro of the replication fork, Cell 129 (2007) 665–679.
[36] D.C. Altieri, Survivin, versatile modulation of cell division and apoptosis in cancer, Oncogene 22 (2003) 8581–8589.
[37] V. Kirkin, S. Joos, M. Zornig, The role of Bcl-2 family members in tumorigenesis, Biochim. Biophys. Acta 1644 (2004) 229–249.
[38] C.A. Heinlein, C. Chang, Androgen receptor in prostate cancer, Endocr. Rev. 25 (2004) 276–308.
[39] M.L. Zhu, N. Kyprianou, Androgen receptor and growth factor signaling cross-talk in prostate cancer cells, Endocr. Relat. Cancer 15 (2008) 841–849.
[40] L.M. Rozan, W.S. El-Deiry, p53 downstream target genes and tumor suppression: a classical view in evolution, Cell Death Differ. 14 (2007) 3–9.
[41] K. Polyak, Y. Xia, J.L. Zweier, K.W. Kinzler, B. Vogelstein, A model for p53-induced apoptosis, Nature 389 (1997) 300–305.
[42] S. Yasuda, S. Yogosawa, Y. Izutani, Y. Nakamura, H. Watanabe, T. Sakai, Cucurbitacin B induces G(2) arrest and apoptosis via a reactive oxygen species-dependent mechanism in human colon adenocarcinoma SW480 cells, Mol. Nutr. Food Res. (2009).
[43] J.P. Lin, J.S. Yang, C.C. Lu, J.H. Chiang, C.L. Wu, J.J. Lin, H.L. Lin, M.D. Yang, K.C. Liu, T.H. Chiu, J.G. Chung, Rutin inhibits the proliferation of murine leukemia WEHI-3 cells in vivo and promotes immune response in vivo, Leuk. Res. 33 (2009) 823–828.
[44] H. Luo, B.H. Jiang, S.M. King, Y.C. Chen, Inhibition of cell growth and VEGF expression in ovarian cancer cells by flavonoids, Nutr. Cancer 60 (2008) 800–809.
[45] C. Martinez Conesa, V. Vicente Ortega, M.J. Yanez Gascon, M. Alcaraz Banos, M. Canteras Jordana, O. Benavente-Garcia, J. Castillo, Treatment of metastatic melanoma B16F10 by the flavonoids tangeretin, rutin, and diosmin, J. Agric. Food Chem. 53 (2005) 6791–6797.
[46] M. Zhang, N.S. Hettiarachchy, R. Horax, P. Chen, K.F. Over, Effect of maturity stages and drying methods on the retention of selected nutrients and phytochemicals in bitter melon (*Momordica charantia*) leaf, J. Food Sci. 74 (2009) C441–448.
[47] C.S. Muir, J. Nectoux, J. Staszewski, The epidemiology of prostatic cancer. Geographical distribution and time-trends, Acta Oncol. 30 (1991) 133–140.

Organ Specific Gst-pi Expression of the Metastatic Androgen Independent Prostate Cancer Cells in Nude Mice

Taku Naiki,[1,2] Makoto Asamoto,[1]* Naomi Toyoda-Hokaiwado,[1] Aya Naiki-Ito,[1] Keiichi Tozawa,[2] Kenjiro Kohri,[2] Satoru Takahashi,[1] and Tomoyuki Shirai[1]

[1]*Department of Experimental Pathology and Tumor Biology, Nagoya City University, Graduate School of Medical Sciences, Nagoya, Japan*

[2]*Department of Nephro-urology, Nagoya City University, Graduate School of Medical Sciences, Nagoya, Japan*

BACKGROUND. Elucidating the mechanisms of metastasis in prostate cancer, particularly to the bone, is a major issue for treatment of this malignancy. We previously reported that an androgen-independent variant had higher expression of glutathione S-transferase pi (Gst-pi) compared with a parent androgen-dependent transplantable rat prostate carcinoma which was established from the transgenic rat for adenocarcinoma of the prostate (TRAP).

METHODS. A new cell line, PCai1, was established from the androgen-independent tumor and investigated its metastatic potential in nude mice. The tumorigenesis of PCai1 cells in vivo was studied by subcutaneous transplantations into nude mice. The growth in the micro-environment of the prostate was studied by orthotopic transplantation of PCai1 cells into nude mice. The metastatic potential of PCai1 cells was studied by tail vein injections. Effects of *Gst-pi* knocked down were analysis in PCai1 cells.

RESULTS. PCai1 frequently formed metastatic lesions in the lung and lymph nodes after orthotopic implantation in the prostate. Intravenous injections of PCai1, metastasis to lung and bone were obvious. PCai1 had strong expression for Gst-pi, therefore we tried knocked down *Gst-pi*. *Gst-pi*-siRNA in vitro significantly suppressed cell proliferation rate. In addition, high levels of intracellular reactive oxygen species (ROS) were recognized in the *Gst-pi* knockout.

CONCLUSIONS. Gst-pi expression of the prostate cancers are dependent on metastatic site, and that Gst-pi has an important role in adapting prostate cancer for growth and metastasis involving an alteration of ROS signals. *Prostate 72: 533–541, 2012.* © 2011 Wiley Periodicals, Inc.

KEY WORDS: **prostate cancer; metastasis; Gst-pi; rats; cell line**

INTRODUCTION

Prostate cancer is one of the most frequently diagnosed cancers in the Western world [1]. Because prostate cancer development is initially androgen dependent, the basic therapeutic strategy has been the deprivation of androgens [2]. However, most tumors ultimately relapse after a period of initial response to this therapy and progress to castration-resistant prostate cancer (CRPC), for which effective therapeutic procedures are extremely limited. Administration of docetaxel has been established as a new standard of chemotherapy for CRPC patients [3–5]. However, it is not curative, and optimal timing of administration remains controversial. Consequently, there is a need

Grant sponsor: Ministry of Education, Culture, Sports Science and Technology of Japan; Grant sponsor: Ministry of Health, Labor and Welfare of Japan; Grant sponsor: Ono Pharmaceutical Co., Ltd.

Disclosure: There are no potential conflicts of interest.

Naomi Toyoda-Hokaiwado's present address is Division of Genetics and Mutagenesis, National Institute of Health Sciences, Tokyo, Japan.

*Correspondence to: , Dr. Makoto Asamoto, MD, PhD, Department of Experimental Pathology and Tumor Biology, Nagoya City University, Graduate School of Medical Sciences, Kawasumi 1, Mizuho-cho, Mizuho-ku 467-8601, Nagoya, Japan.
E-mail: masamoto@med.nagoya-cu.ac.jp

Received 7 January 2011; Accepted 15 June 2011
DOI 10.1002/pros.21455
Published online 11 July 2011 in Wiley Online Library (wileyonlinelibrary.com).

for exploration of new therapeutic strategies targeting detailed molecular mechanisms for the development of castration resistance in prostate cancer.

The generation of suitable in vivo models is essential to gain a better understanding of the processes associated with the development and progression of prostate cancer [6,7]. We previously reported on the transgenic rat model for adenocarcinoma of the prostate (TRAP) model [8], which features the introduction of the SV40 T antigen (SV40 Tag) gene under probasin control. In this model, complete androgen-dependent prostate adenocarcinomas developed in 100% of animals by 15 weeks of age [8–10]. These tumors were transplantable into the subcutis of nude mice. The transplanted tumors expressing androgen receptor (AR) regressed soon after the mice were castrated, but resumed growth under androgen depletion 12 weeks later. As the sequential changes of the xenograft resemble the clinical behavior of prostate cancer, this model may provide an excellent system to study the mechanisms associated with castration-resistant progression of prostate cancer and to evaluate new modalities for CRPC [11]. The androgen-independent prostate tumors established under such an experimental condition were subjected to cDNA microarray analysis which showed that glutathione S-transferase pi (*Gst-pi*) was overexpressed compared to the androgen-dependent tumors. Glutathione S-transferase pi (*GST-pi*) was also found to be overexpressed in the androgen-independent prostate cancer cell line, PC3 [11]. The suppression of GST-pi expression by siRNA inhibited tumor growth after subcutaneous transplantation of PC3 cells in nude mice [11].

A major component involved in the maintenance of reduction-oxidation (redox) balance in the cell is the glutathione redox system. Methods of inactivating *GST-pi* had been identified in almost all of the prostate cancer cases examined by Nelson et al. [12]. Since then, many reports have described the relations between *GST-pi* and androgen-dependent prostate cancer, and loss of the expression of their promoter sequences by methylation was found as an early event in human prostate carcinogenesis [13,14]. Therefore, a sensitive balance appears to exist between the oxidant and antioxidant components of the cells and their regulatory mechanisms in developing a malignant state in prostate tissue.

Redox reactions that generate reactive oxygen species (ROS) such as hydrogen peroxide, superoxide, and hydroxyl-free radicals have been identified as important chemical mediators in the regulation of signal transduction processes involved in cell growth and differentiation and have been reviewed [15–17]. ROS content is relatively higher in prostate epithelial cells than in most other tissues [18]. Direct evidence linking ROS with an increase in tumor development in the prostate has been established [19,20]. Previous studies highlighted the altered pro-oxidant–antioxidant status in prostatic tissue, and also in cell lines where the imbalance between these antagonists played a major role in the initiation of prostate carcinogenesis [21]. However, only few reports are available that describes interactions between androgen-independent prostate cancer and ROS. Moreover, no report addressed the mechanism using a cell line with a high metastatic potential in vivo.

In the present study, new androgen-independent prostate cancer cells were established which metastasized when transplanted into nude mice. The expression and function of Gst-pi in each metastatic site of the androgen-independent prostate cancer cells were studied.

MATERIALS AND METHODS

A New Androgen-Independent Prostate Cancer Cell Line

Cultures were initiated by mechanical disruption of the androgen-independent prostate tumor in nude mice [11] followed by enzymatic digestion with trypsin for 24 hr at 37°C. The resulting cells were incubated in DMEM (Nissui, Tokyo, Japan) with 10% heat-inactivated fetal bovine serum (FBS) (Equitech-Bio, Kerrville, TX). After 10 months passage and incubation, the surviving cells were selected and the cells that had the SV40 Tag expressions by RT-PCR were subcloned. Furthermore, the surviving cells in the androgen depleted medium containing 10% charcoal-stripped- (CS-) FBS (Hyclone) were selected, and one of these cell lines, named PCai1, which was androgen-independent cell line in vitro was used in our experiments. All cell cultures were maintained at 37°C in a humidified incubator with an atmosphere of 5% CO_2/95% air.

In Vivo Tumor Growth

Six-week-old male KSN/nu-nu nude mice were obtained from Nippon SLC. Mice were maintained in plastic cages on hardwood chips in an air-conditioned, pathogen-free animal room at 22 ± 2°C and 50% humidity with 12:12 hr light/dark cycle. All animal experiments were performed under protocols approved by the Institutional Animal Care and Use Committee of Nagoya City University School of Medical Sciences.

Subcutaneous transplantation of PCai1 cells. The tumorigenesis of PCai1 cells in vivo was studied by

subcutaneous transplantations into nude mice. PCai1 cells were cultured in T-75 flasks to confluence, trypsinized, and enumerated. Under isoflurane anesthesia four mice were surgically castrated and after 3 days, 1×10^5 PCai1 cells were injected subcutaneously into four normal and four castrated mice. Tumor sizes were calculated every 2 weeks, and mice were sacrificed 10 weeks after the implantation.

Orthotopic transplantation of PCai1 cells. The growth in the microenvironment of the prostate was studied by orthotopic transplantation of PCai1 cells into nude mice. Under isoflurane anesthesia, 5 of 10 nude mice were surgically castrated. After 3 days, 5×10^5 PCai1 cells were implanted into the lateral lobe of the prostate in both castrated and non-castrated mice. Two mice of each group were sacrificed 2 weeks after the injection. The study was terminated until become when the mice appeared moribund. After sacrifice, the orthotopic growth of the tumor and metastases in the para-aortic and bilateral inguinal lymph nodes, lung and systemic bone tissues were investigated histopathologically, as well as performing immunohistochemical analyses for AR, SV40 Tag, and Gst-pi.

Tail vein injection of PCai1 cells. The metastatic potential of PCai1 cells was studied by tail vein injections. Seven $\times 10^6$ cells were injected into the tail veins of 10 mice under anesthesia. At 5 and 9 weeks after the injections, the mice were sacrificed and the metastases in the para-aortic and bilateral inguinal lymph nodes, lung and systemic bone were investigated macroscopically and by immunohistochemical staining.

Histopathological Analysis

The transplants and metastatic tumors were fixed in 10% buffered formalin and embedded in paraffin. For bone metastases, specimens were treated with sterile decalcification solution for 48 hr prior to paraffin embedding. Serial (4 □m thick) sections were prepared. For immunohistochemical analysis, deparaffinized sections of the tissues were incubated with 1:1,000 diluted anti-Gst-pi (MBL, Nagoya, Japan), 1:100 diluted anti-AR (Santa Cruz Biotechnology, Inc., CA), 1:500 diluted SV40 Tag antibody (PharMingen, San Diego, CA). Antibody binding was visualized by a conventional immunostaining method using an autoimmunostaining apparatus (HX System, Ventana, Tucson, AZ).

RNA Preparation and Quantitative RT-PCR for Gst-pi and Gapdh

Total RNA was extracted using Isogen (Nippon Gene, Tokyo, Japan). One microgram sample was converted to complementary DNA with avian myoblastosis virus reverse transcriptase and oligo dT primers (TaKaRa, Otsu, Japan) in 20 □l of reaction mixture and 2 □l aliquots were subjected to quantitative polymerase chain reaction in 20 □l reactions using SYBR Premix Ex Taq™ (TaKaRa) and a Light Cycler apparatus (Roche Diagnostics, Mannheim, Germany). The fluorescence intensity of double-strand-specific SYBR Green 1, reflecting the amount of formed polymerase chain reaction product, was monitored at the end of each elongation step. Cyclophilin messenger RNA levels were employed to normalize for the 5′ sample complementary DNA content. Primer sequences for rat *Gst-pi* were 5′-GCTCTTTAGGGCTTTATGGG-3′ and 5′-CTGTTTACCATTGCCGTTGA-3′, and 5′-GCATCCTGCACCACCAACTG-3′ and 5′-GCCTGCTTCACCACCTTCTT-3′ for glyceraldehyde-3-phosphate dehydrogenase (*Gapdh*). Initial denaturation was at 95°C for 5 sec, annealing was at 55°C for 15 sec, and subsequently elongation was at 72°C for 30 sec. Gapdh mRNA levels were used for normalizing the sample cDNA content of PCai1 cells.

siRNA Transfection and Cell Growth Assay In Vitro

Stealth Select RNAi targeting rat *Gst-pi* sequences were obtained from Invitrogen. PCai1 cells (2×10^5) were seeded in six-well plates and transfected with 30 nM siRNA using LipofectAMINE RNAiMAX (Invitrogen) according to the manufacturer's protocol. Silencer negative control #1 siRNA (Invitrogen) with no significant homology to any known rat genes was used as a negative control siRNA. The ability of siRNA to silence the expression level of *Gst-pi* mRNA was checked on the second day after transfection. For monitoring growth inhibition, cells were trypsinized ($n = 4$) on days 3 and 5, and then the cell numbers were counted.

In Vivo Tumor Growth Analysis by Using siRNA for ⊠⊠⊠

Twenty-four hours after *Gst-pi* siRNA transfection by lipofectamine in T-75 flask, PCai1 cells were trypsinized and suspended in the DMEM media without serum, and 1×10^5/mouse cells were injected subcutaneously into five normal and five castrated nude mice. Negative control siRNA treated cells were also injected into normal and castrated mice for controls. Tumor volume was calculated every week, and 3 weeks after inoculation, the four groups of mice

were sacrificed and the final tumor volumes were measured in each group.

Western Blotting for Gst-pi and AR

Cells were lysed in SDS buffer and 10 □l were resolved on 12% polyacrylamide gels and transferred to Hybond ECL (GE Healthcare). Gst-pi and AR expression levels were assessed with the same antibody used for immunohistochemical staining. Beta actin expression was evaluated to confirm equal amount of protein loadings by monoclonal anti-beta-actin (Sigma, St. Louis, MO).

Cell Proliferation Assay After Dihydrotestosterone (DHT) Treatment

PCai1 cells were pretreated with medium containing CS-FBS for 2 weeks, and cell proliferation was measured in response to dihydrotestosterone (DHT) (Wako, Tokyo, Japan) treatments. PCai1 cells (5×10^4) were re-seeded in 96-well plates and treated with DHT from 10^{-5} to 10^5 nM in CS-FBS medium. Twenty-four hours after incubation, 10 □l/well of Cell Proliferation Reagent WST-1 (Roche, Basal, Switzerland) was added to the cells. Two hours after incubation, increase in fluorescence was measured by Spectrafluor Plus (Wako). The mean fluorescence intensity at 430 nm was calculated.

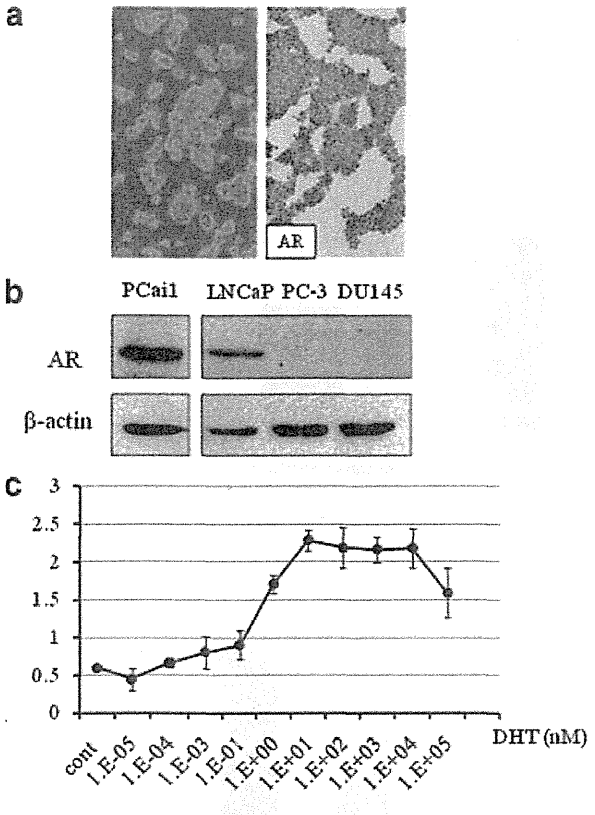

Fig. 1.

Measurement of Intracellular ROS Level

After pretreatment with DMEM without phenol red for 24 hr, 1×10^4 PCai1 cells were re-seeded in 96-well plates for 24 hr. The cells were then treated with 100 □g/ml 5-(and-6-)-chloromethyl-2′, 7′-dichlorodihydrofluorescein diacetate, acetyl ester (CM-H_2DCFDA) dye (Invitrogen). After 45 min incubation in the dark, levels of specific fluorescence were measured by Spectrafluor Plus. The data were normalized by the proliferation rate measured by the WST-1 assay.

Ethacrynic Acid Treatment in PCai1 Cells

To examine direct effects of Gst-pi on production of ROS or cell proliferation, PCai1 cells were treated with ethacrynic acid (EA) (Sigma), glutathione S-transferase pi inhibitor. Briefly, PCai1 cells were pretreated with phenol-free medium containing 10% FBS for 2 weeks, and cell proliferation and intracellular ROS were measured in response to EA treatments. PCai1 cells (1×10^5) were seeded in six-well plates, and exposed to 1 □M, 10 □M of EA. Cells were

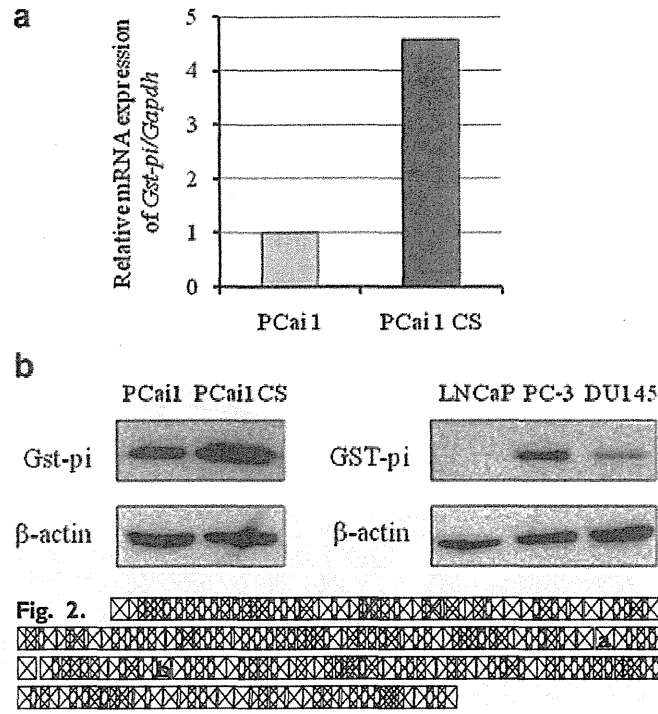

Fig. 2.

counted on days 3 and 5, and measurement of ROS level was performed as described above.

RESULTS

Establishment of an Androgen-Independent Prostate Cancer Cell Line

Our newly established androgen independent prostate cancer cell line, PCai1 (Fig. 1a), can survive in androgen-free DMEM with 10% CS-FBS. The cells showed intense nuclear immunohistochemical staining for AR in normal medium containing androgen (Fig. 1a). PCai1 and a human prostate cancer cell line LNCaP showed similar expressions of AR (Fig. 1b). The WST-1 assay revealed that cell growth was enhanced by 1–10 nM of DHT (Fig. 1c), so this cell line was androgen-independent and androgen-sensitive.

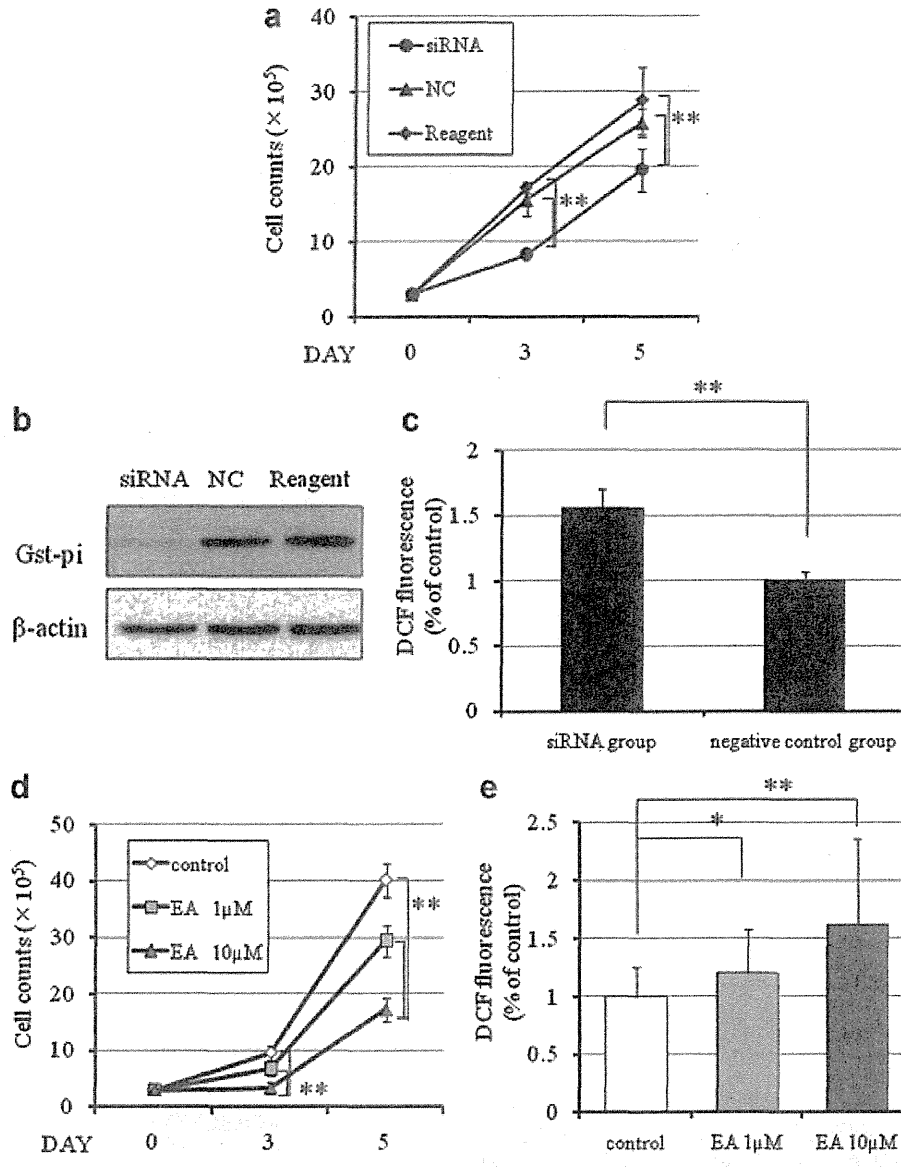

Fig. 3. [illegible] Gst-pi [illegible] *P [illegible] Gst-pi [illegible] Gst-pi [illegible] Gst-pi [illegible] *P [illegible] *P [illegible] *P [illegible] *P [illegible]

The Gst-pi Expression in PCai1 Cells

PCai1 cells in normal medium had stable expressions of Gst-pi in mRNA and protein levels. When PCai1 cells were cultured in CS-FBS medium, Gst-pi expressions were enhanced in mRNA and protein levels (Fig. 2). As reported previously [11], in human prostate cancer cells GST-pi expression was higher in the androgen-independent cell lines (PC3, DU145) compared with an androgen-dependent cell line (LNCaP). These results indicate that Gst-pi expression is higher in androgen-independent prostate cancer than those that are androgen-dependent.

[illegible]siRNA Transfection and ROS Signals

To examine the role of Gst-pi expression for ROS signaling in PCai1 cells, *Gst-pi* expression was attenuated by RNAi. The suppression of proliferation of PCai1 cells in CS-FBS medium was statistically significant in *Gst-pi*-siRNA treated cells, but not in *Gst-pi*-negative control cells (Fig. 3a). Western blot analysis revealed Gst-pi protein expression has been inhibited by siRNA for 5 days after transfection (Fig. 3b). DCFH assay revealed that the intracellular ROS levels were significantly higher in the *Gst-pi*-siRNA treatment group than in *Gst-pi*-negative control group (Fig. 3c). Next, to examine whether Gst-pi directly affects modification of cell proliferation and production of ROS, PCai1 cells were treated with EA, a glutathione S-transferase pi inhibitor. As expected, proliferation of PCai1 was significantly inhibited by 1 and 10 [illegible]M EA compared with the non-treated control (Fig. 3d). Intracellular ROS levels were also significantly higher in the EA treatment group in a concentration-dependent manner (Fig. 3e).

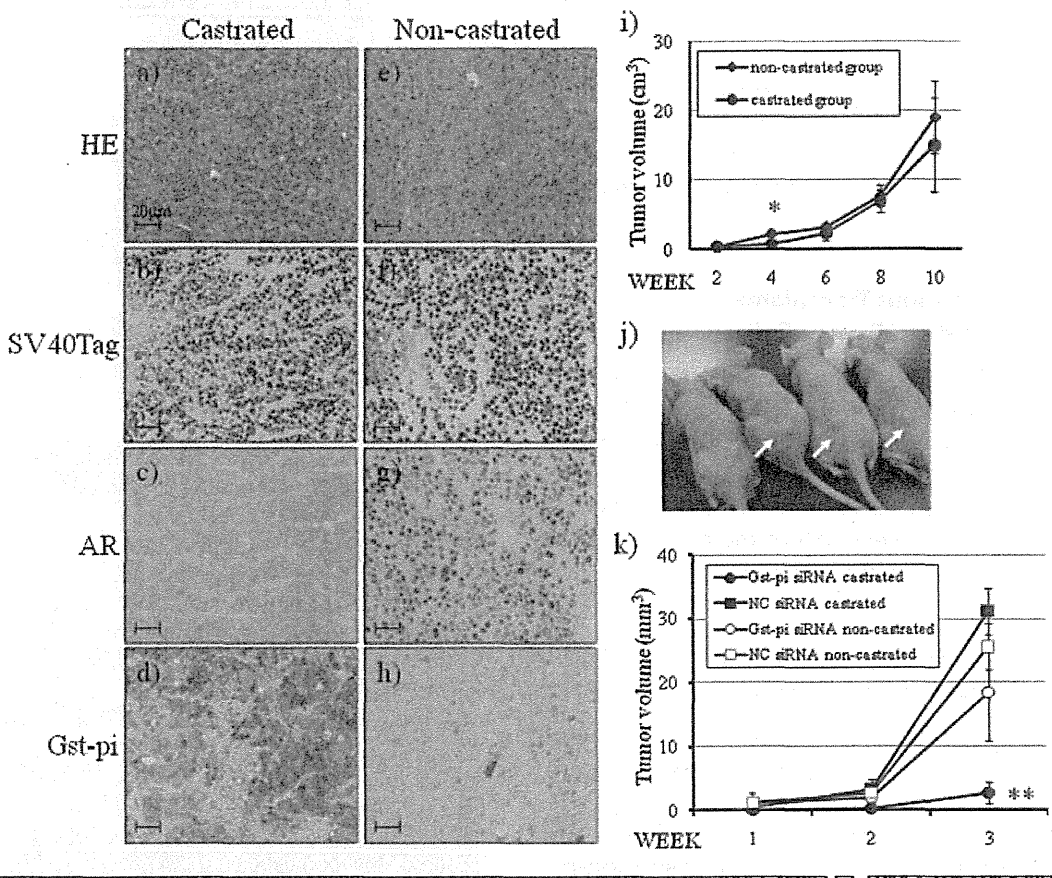

Fig. 4. [illegible]

Prostate Cancer Subcutaneous Tumor Model

For investigation of tumorigenesis, PCai1 cells were transplanted subcutaneously in nude mice. Successful growth was seen in both castrated and non-castrated mice. The tumor sizes between the two groups lacked significance (Fig. 4i). Transplanted PCai1 cells had strong nuclear SV40 Tag expression, and demonstrated intense nuclear AR staining in the non-castrated group. In contrast, AR expression had changed from the nucleus to the cytoplasm in the castrated mice indicated not functional (Fig. 4a–h).

Prostate Cancer Orthotopic Transplanted Model

Whether or not they were castrated, the PCai1 cells grew in the prostate site in nude mice forming tumors which frequently metastasized to the lung and lymph nodes in nude mice (Fig. 5a–c and Table I). However, the mice could not survive more than 6 weeks because of urinary retention resulting from the tumor growth. Histopathologically, the prostate tumors in mice had similar characteristics as poorly differentiated prostate adenocarcinomas in human.

Intravenous Transplanted Prostate Cancer Cells

With injections of PCai1 cells into the tail veins of nude mice, metastatic tumors were frequently observed in the lungs and bones (Fig. 5g,h and Table I). Immunocytochemically, the SV40 Tag signals were intense in nuclei of PCai1 cells in vitro and in vivo of the metastasized tumor cells. All of the bone metastases were found in the lumbar vertebrae.

Regulation of Castration-Resistant Cell Growth of PCai1 by Gst-pi In Vivo

In the subcutaneous PCai1 tumors, Gst-pi expression was significantly higher in the castrated group (Fig. 4d) than in the non-castrated group (Fig. 4h) without changes in expressions of SV40 Tag (Fig. 4b,f). To evaluate roles of Gst-pi in castration-resistant cell proliferation, *Gst-pi* siRNA transfected PCai1 cells were transplanted subcutaneously in castrated or normal nude mice. Knock down of *Gst-pi* expression of PCai1 significantly inhibited tumor growth of PCai1 compared to negative controls in castrated mice. On the other hand, *Gst-pi* expression did not affect tumor growth in non-castrated mice (Fig. 4j,k).

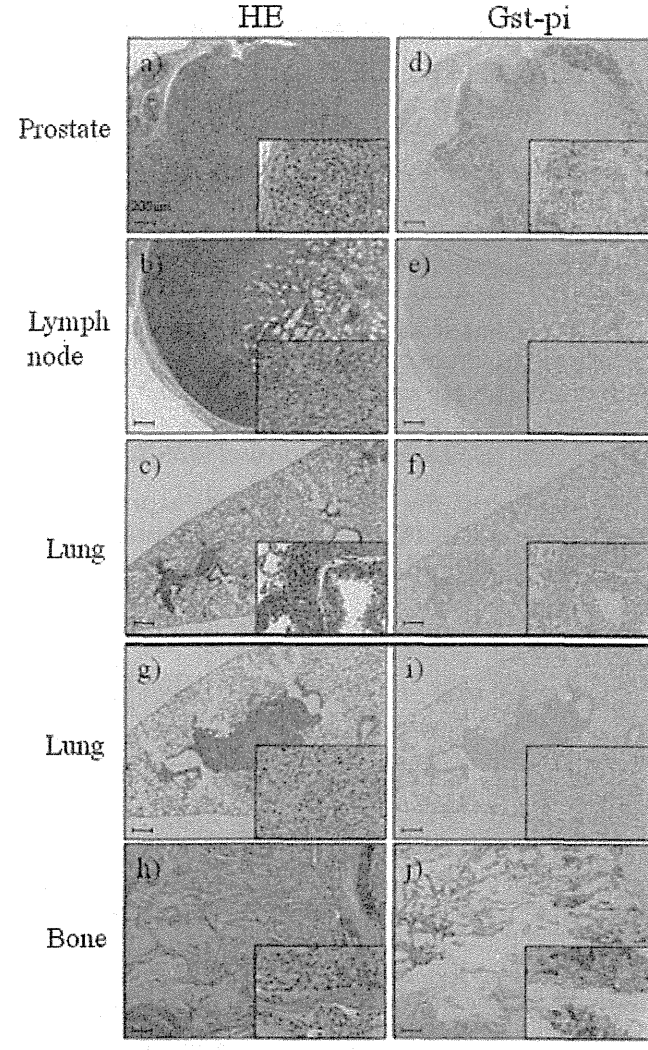

Fig. 5.

Immunohistochemical Analysis for Gst-pi in Prostate Cancer Metastatic Models

In the orthotopic in vivo model, Gst-pi showed high expression in the prostate, but no expression in

TABLE I. Frequency of Metastasis by PCai1 Cell Line

Transplantation	Castration	Sacrifice (weeks)	No. of mice	Primary tumor (%)	Metastasis (%)		
					Lymph node	Lung	Bone
Subcutaneous	–	10	4	100	–	–	–
	+	10	4	100	–	–	–
Orthotopic (prostate)	–	2	2	100	0	0	0
		5	3	100	100	33	0
	+	2	2	50	0	0	0
		6	3	100	100	75	0
Tail vein	–	5	5	–	40	80	20
		9	5	–	80	100	40

metastatic sites of lung and lymph nodes (Fig. 5d–f). However, the tumor cells injected in the tail veins resulted in tumor masses in the bone with high Gst-pi expressions (Fig. 5j). In lung (Fig. 5i) and lymph nodes, metastatic tumors did not express Gst-pi similar to that observed for lymph nodes and lung metastatic cells in the orthotopic model. These observations suggest that Gst-pi has different expression levels according to metastatic sites.

DISCUSSION

To elucidate the mechanisms of prostate cancer progression, and metastasis, physiologically relevant models are essential for understanding the human disease. Prostate cancer in the TRAP model showed marked epithelial proliferation with formation of irregular glands and luminal bridging to give a cribriform pattern, and their nuclei demonstrated enlargement and severe atypia [8]. These lesions are compatible with what are seen in human adenocarcinomas. Because of the biological complexity, bone metastatic models for prostate cancer are limited [22]. In the bone metastatic sites in our model, osteolytic areas mixed with osteoblastic areas were recognized that are similar to human cases. Therefore, our model may contribute useful information for understanding the mechanisms of prostate cancer metastasis.

The intracellular redox state balances oxidant production and antioxidant capacity of the cells based on a variety of antioxidant enzymes such as superoxide dismutase, catalase, glutathione peroxidase, and GST-pi. The glutathione redox system acts in concert to provide a coordinated network of protection against ROS accumulation and oxidative damage [23–25]. GST-pi is directly responsible for the elimination of electrophilic oxidants [23,24] especially in cancer cells characterized by rapid proliferating activity and with massive endogenous production of ROS [17].

GST-pi was usually silenced by methylation in human prostate cancer cells. However, with the acquisition of androgen-independency, our present data suggested that prostate cancer might have protective mechanisms against ROS by GST-pi signals. In our previous data, the expression level of *Gst-pi* was higher in transplantable tumors that were androgen-independent than in those that were androgen-dependent [11]. PCai1 cells in androgen-free medium had higher protein expressions of Gst-pi than in androgen-containing medium, and PCai1 tumors had higher Gst-pi expressions in castrated mice than in control mice with subcutaneous tumors and orthotopic prostate tumors in vivo. These data suggest that Gst-pi can regulate cancer cell growth by adapting to the environment. Silencing of *Gst-pi* caused significant growth inhibition of PCai1 cells, and DCFH assay revealed that intracellular ROS was significantly elevated in *Gst-pi*-siRNA and Gst-pi inhibitor treated groups. These results suggested that Gst-pi plays an important role in cell growth against ROS in PCai1 cells.

According to previous reports [26,27], the level of Gst-pi can change in response to general cellular stress. Therefore, to establish that the high expression of Gst-pi was not a reflection of cellular stress, PCai1 transplantation was performed in castrated and normal nude mice with iRNA strategy for *Gst-pi*. As a result, tumor growth of PCai1 was significantly inhibited by silencing *Gst-pi* in castrated nude mice. Therefore, Gst-pi may be necessary in androgen-independent cell growth.

Immunohistochemical analysis revealed that Gst-pi expression in subcutaneous tumors and prostate tumors in orthotopic transplants was significantly increased by castration. On the other hand, lymph nodes and lung metastatic lesions had no expression of Gst-pi. Interestingly, Gst-pi expression of the bone metastatic lesions had higher expression levels than other lesions. These findings show that Gst-pi may be

a novel therapeutic protein that can be targeted for bone metastasis.

Our newly established prostate cancer cell line PCai1, derived from the well-characterized TRAP model, may be valuable in an animal model to study the progression and metastasis of prostate cancer, and for preclinical tests of new and innovative therapeutic agents.

In summary, using our newly established prostate cancer cell line PCai1 and the metastatic models, Gst-pi expressions were shown to have important roles in prostate cancer growth and organ specific metastasis.

ACKNOWLEDGMENTS

This work was supported in part by a Grant-Aid from the Ministry of Education, Culture, Sports Science and Technology of Japan, by a Grand-Aid for Cancer Research from the Ministry of Health, Labor and Welfare of Japan, and by a Grant-Aid for Ono Pharmaceutical Co., Ltd.

REFERENCES

1. Gronberg H. Prostate cancer epidemiology. Lancet 2003; 361(9360):859–864.
2. Huggins C. Endocrine-induced regression of cancers. Cancer Res 1967;27(11):1925–1930.
3. Petrylak DP, Tangen CM, Hussain MH, Lara PN Jr, Jones JA, Taplin ME, Burch PA, Berry D, Moinpour C, Kohli M, Benson MC, Small EJ, Raghavan D, Crawford ED. Docetaxel and estramustine compared with mitoxantrone and prednisone for advanced refractory prostate cancer. N Engl J Med 2004;351(15): 1513–1520.
4. Schurko B, Oh WK. Docetaxel chemotherapy remains the standard of care in castration-resistant prostate cancer. Nat Clin Pract Oncol 2008;5(9):506–507.
5. Oh WK, Kantoff PW. Docetaxel (Taxotere)-based chemotherapy for hormone-refractory and locally advanced prostate cancer. Semin Oncol 1999;26(5 Suppl 17):49–54.
6. Shirai T. Significance of chemoprevention for prostate cancer development: Experimental in vivo approaches to chemoprevention. Pathol Int 2008;58(1):1–16.
7. Shirai T, Takahashi S, Cui L, Futakuchi M, Kato K, Tamano S, Imaida K. Experimental prostate carcinogenesis—Rodent models. Mutat Res 2000;462(2–3):219–226.
8. Asamoto M, Hokaiwado N, Cho YM, Takahashi S, Ikeda Y, Imaida K, Shirai T. Prostate carcinomas developing in transgenic rats with SV40 T antigen expression under probasin promoter control are strictly androgen dependent. Cancer Res 2001;61(12):4693–4700.
9. Said MM, Hokaiwado N, Tang M, Ogawa K, Suzuki S, Ghanem HM, Esmat AY, Asamoto M, Refaie FM, Shirai T. Inhibition of prostate carcinogenesis in probasin/SV40 T antigen transgenic rats by leuprorelin, a luteinizing hormone-releasing hormone agonist. Cancer Sci 2006;97(6):459–467.
10. Tang M, Ogawa K, Asamoto M, Hokaiwado N, Seeni A, Suzuki S, Takahashi S, Tanaka T, Ichikawa K, Shirai T. Protective effects of citrus nobiletin and auraptene in transgenic rats developing adenocarcinoma of the prostate (TRAP) and human prostate carcinoma cells. Cancer Sci 2007;98(4):471–477.
11. Hokaiwado N, Takeshita F, Naiki-Ito A, Asamoto M, Ochiya T, Shirai T. Glutathione S-transferase Pi mediates proliferation of androgen-independent prostate cancer cells. Carcinogenesis 2008;29(6):1134–1138.
12. Nelson WG, De Marzo AM, DeWeese TL. The molecular pathogenesis of prostate cancer: Implications for prostate cancer prevention. Urology 2001;57(4 Suppl 1):39–45.
13. Pathak S, Singh R, Verschoyle RD, Greaves P, Farmer PB, Steward WP, Mellon JK, Gescher AJ, Sharma RA. Androgen manipulation alters oxidative DNA adduct levels in androgen-sensitive prostate cancer cells grown in vitro and in vivo. Cancer Lett 2008;261(1):74–83.
14. Miyake H, Hara I, Kamidono S, Eto H. Oxidative DNA damage in patients with prostate cancer and its response to treatment. J Urol 2004;171(4):1533–1536.
15. Finkel T, Holbrook NJ. Oxidants, oxidative stress and the biology of ageing. Nature 2000;408(6809):239–247.
16. Nose K. Role of reactive oxygen species in the regulation of physiological functions. Biol Pharm Bull 2000;23(8):897–903.
17. Sauer H, Wartenberg M, Hescheler J. Reactive oxygen species as intracellular messengers during cell growth and differentiation. Cell Physiol Biochem 2001;11(4):173–186.
18. Feig DI, Reid TM, Loeb LA. Reactive oxygen species in tumorigenesis. Cancer Res 1994;54(7 Suppl):1890s–1894s.
19. Dakubo GD, Parr RL, Costello LC, Franklin RB, Thayer RE. Altered metabolism and mitochondrial genome in prostate cancer. J Clin Pathol 2006;59(1):10–16.
20. Chomyn A, Attardi G. MtDNA mutations in aging and apoptosis. Biochem Biophys Res Commun 2003;304(3):519–529.
21. Ripple MO, Henry WF, Rago RP, Wilding G. Prooxidant-antioxidant shift induced by androgen treatment of human prostate carcinoma cells. J Natl Cancer Inst 1997;89(1):40–48.
22. Singh AS, Figg WD. In vivo models of prostate cancer metastasis to bone. J Urol 2005;174(3):820–826.
23. Finkel T. Oxidant signals and oxidative stress. Curr Opin Cell Biol 2003;15(2):247–254.
24. Kohen R, Nyska A. Oxidation of biological systems: Oxidative stress phenomena, antioxidants, redox reactions, and methods for their quantification. Toxicol Pathol 2002;30(6):620–650.
25. Oberley LW, Buettner GR. Role of superoxide dismutase in cancer: A review. Cancer Res 1979;39(4):1141–1149.
26. Morel F, Fardel O, Meyer DJ, Langouet S, Gilmore KS, Meunier B, Tu CP, Kensler TW, Ketterer B, Guillouzo A. Preferential increase of glutathione S-transferase class alpha transcripts in cultured human hepatocytes by phenobarbital, 3-methylcholanthrene, and dithiolethiones. Cancer Res 1993;53(2):231–234.
27. Thimmulappa RK, Mai KH, Srisuma S, Kensler TW, Yamamoto M, Biswal S. Identification of Nrf2-regulated genes induced by the chemopreventive agent sulforaphane by oligonucleotide microarray. Cancer Res 2002;62(18):5196–5203.

The Prostate 72:1559–1572 (2012)

Therapeutic Targeting of Angiotensin II Receptor Type I to Regulate Androgen Receptor in Prostate Cancer

Satoru Takahashi,[1]* Hiroji Uemura,[2] Azman Seeni,[1,3] Mingxi Tang,[1,4] Masami Komiya,[1] Ne Long,[1] Hitoshi Ishiguro,[2] Yoshinobu Kubota,[2] and Tomoyuki Shirai[1]

[1]*Department of Experimental Pathology and Tumor Biology, Nagoya City University Graduate School of Medical Sciences, Nagoya, Japan*
[2]*Department of Urology, Yokohama City University Graduate School of Medicine, Yokohama, Japan*
[3]*Advanced Medical and Dental Institute, Universiti Sains Malaysia, Pinang, Malaysia*
[4]*Department of Pathology, Luzhou Medical College, Sichuan, China*

BACKGROUND. With the limited strategies for curative treatment of castration-resistant prostate cancer (CRPC), public interest has focused on the potential prevention of prostate cancer. Recent studies have demonstrated that an angiotensin II receptor blocker (ARB) has the potential to decrease serum prostate-specific antigen (PSA) level and improve performance status in CRPC patients. These facts prompted us to investigate the direct effects of ARBs on prostate cancer growth and progression.

METHODS. Transgenic rat for adenocarcinoma of prostate (TRAP) model established in our laboratory was used. TRAP rats of 3 weeks of age received ARB (telmisartan or candesartan) at the concentration of 2 or 10 mg/kg/day in drinking water for 12 weeks. In vitro analyses for cell growth, ubiquitylation or reporter gene assay were performed using LNCaP cells.

RESULTS. We found that both telmisartan and candesartan attenuated prostate carcinogenesis in TRAP rats by augmentation of apoptosis resulting from activation of caspases, inactivation of p38 MAPK and down-regulation of the androgen receptor (AR). Further, microarray analysis demonstrated up-regulation of estrogen receptor β (ERβ) by ARB treatment. In both parental and androgen-independent LNCaP cells, ARB inhibited both cell growth and AR-mediated transcriptional activity. ARB also exerted a mild additional effect on AR-mediated transcriptional activation by the ERβ up-regulation. An intervention study revealed that PSA progression was prolonged in prostate cancer patients given an ARB compared with placebo control.

CONCLUSION. These data provide a new concept that ARBs are promising potential chemopreventive and chemotherapeutic agents for prostate cancer. *Prostate 72: 1559–1572, 2012.* © 2012 Wiley Periodicals, Inc.

KEY WORDS: **angiotensin II receptor type 1; prostate cancer; androgen receptor; transgenic rat; intervention study**

Additional supporting information may be found in the online version of this article.

Grant sponsor: Ministry of Health, Labour and Welfare of Japan; Grant sponsor: Society for Promotion of Pathology of Nagoya, Japan; Grant sponsor: Ministry of Education, Culture, Science and Technology of Japan; Grant sponsor: Umehara Foundation of Yokohama Medical Group.

S. Takahashi and H. Uemura contributed equally to this work.

Conflict of Interest: None.

*Correspondence to: Dr. Satoru Takahashi, 1 Kawasumi, Mizuho-cho, Mizuho-ku, Nagoya 467-8601, Japan.
E-mail: sattak@med.nagoya-cu.ac.jp

Received 28 September 2011; Accepted 15 February 2012
DOI 10.1002/pros.22505
Published online 16 March 2012 in Wiley Online Library (wileyonlinelibrary.com).

INTRODUCTION

Prostate cancer has become the most common malignancy in men in western countries such as Europe and the United States while its incidence is low in Asian countries. It has been estimated that there will be approximately 240,890 new cases of prostate cancer and 33,720 deaths from prostate cancer in the United States in 2011 [1], and the prevalence of prostate cancer has also been increasing in Japan [2]. Androgen ablation therapy is widely accepted and carried out for prostate cancers because androgens are essential for the development and growth of normal prostate and prostate cancer cells [3]. However, outgrowth of hormone-independent cancer cells occurs within several years and eventually leads to a fatal outcome in many cases [4].

Accumulating evidence suggests that the renin-angiotensin system (RAS) is involved in maintenance of blood pressure as well as progression of various cancers, such as breast, lung, kidney, stomach, colorectum, ovary, and bladder [5]. Angiotensin II is a main effector molecule of the RAS and is an octapeptide hormone with diverse biological activity through binding to typical G protein-coupled receptors, angiotensin II receptor type 1 (AT1R) and type 2 (AT2R). AT1R is expressed in diverse adult tissues and mediates cell proliferation, migration, angiogenesis, and inflammatory responses via G protein-dependent and independent signaling including the MAPK and STAT signal pathways [6]. AT2R is predominantly expressed at a high level in the fetus, and its expression is low in adult tissues, being detectable in heart, kidney, pancreas, adrenal gland, uterus, ovary, and brain [7]. In contrast to AT1R, AT2R has been shown to exert an antagonistic effect against many AT1R-mediated actions [5,8]. Recent studies have demonstrated that an angiotensin II receptor blocker (ARB) has the potential to decrease serum prostate-specific antigen (PSA) level and improve performance status in some patients with castration-resistant prostate cancer (CRPC) [9,10]. Moreover, expression of AT1R and angiotensinogen in CRPC was significantly higher than that in normal prostate tissue or hormone-naive prostate cancer [11]. These facts prompted us to confirm the direct effects of ARBs on prostate cancer and investigate the mechanisms of their suppression of prostate cancer growth and progression.

We have established a transgenic rat for adenocarcinoma of prostate (TRAP) model bearing a probasin promoter/simian virus 40 (SV40) T antigen construct, which features development of high-grade prostatic intraepithelial neoplasia (PIN) from 4 weeks of age and well-moderately differentiated adenocarcinoma with high incidences by 15 weeks of age [12,13]. These characteristics of TRAP have been shown to be very suitable for evaluation of strategies for chemoprevention and treatment with ARBs in vivo.

Here, we showed that ARBs attenuate prostate cancer development in TRAP rats and androgen receptor (AR)-mediated transcriptional activity in human prostate cancer cells. Also, we showed that an ARB delayed PSA progression in patients with local recurrence after radical prostatectomy clinically.

MATERIALS AND METHODS

Chemicals, Reagents, Plasmids, and Cell Line

Telmisartan was provided by Boehringer Ingelheim (Ingelheim, Germany) and candesartan was from Takeda Pharmaceutical Co. Ltd. (Osaka, Japan). MG132 was purchased from Calbiochem (EMD Biosciences, Inc., San Diego, CA), diarylpropionitrile (DPN) from Tocris Bioscience (Bristol, UK), and biochanin A from Sigma (St. Louis, MO). The PSA promoter reporter construct (pGL3/PSA promoter) was donated by Dr. Chawnshang Chang, University of Rochester Medical Center. An expression vector for human ERβ (pCXN2/ERβ) was provided by Dr. Masami Muramatsu (Saitama Medical University, Japan). To generate an expression vector for FLAG-tagged human AR (pCMVTag/hAR), the human AR open reading frame was amplified by PCR and cloned into the pCMV-Tag2 vector at *Bam*HI/*Xho*I sites. The human prostate cancer cell lines LNCaP (androgen-dependent) and VCaP (androgen-independent), and the non-tumorigenic prostate epithelial cell line RWPE-1 were obtained from the American Type Culture Collection (Manassas, VA). Four androgen-independent (AI) sublines derived from LNCaP were established after seven repeated cycles of incubation using the following culture medium; RPMI1640 containing 10% FBS for 5–7 days or RPMI1640 containing 10% charcoal-stripped FBS for 2–3 weeks. AI sublines were designated AI-1, -5, -5s, and -8, respectively (Fig. S1A,B).

Animals

Male heterozygous TRAP rats established in our laboratory with a Sprague–Dawley genetic background were used in the present study. They were housed at three animals per cage on wood-chip bedding in an air-conditioned animal room at 23 ± 2°C and 50 ± 10% humidity. Food and tap water were available ad libitum.

Experimental Protocol

Experiment 1. A total of 36 heterozygous male TRAP rats of 3 weeks of age were randomly divided into

three groups. Rats in Group 1 as a control received basal diet and tap water. The rats in Groups 2 and 3 continuously received 2 or 10 mg/kg/day telmisartan in drinking water for 12 weeks, respectively.

Experiment 2. A total of 48 heterozygous male TRAP rats of 3 weeks of age were randomly divided into four groups. Rats in Group 1 as a control received basal diet and tap water. The rats in Groups 2–4 continuously received 2 or 10 mg/kg/day candesartan or 10 mg/kg/day telmisartan in drinking water for 12 weeks, respectively.

In both experiments, measurement of blood pressure was performed at weeks 4, 7, and 11, and the experiments were terminated at week 15. The prostate was removed and fixed in formalin. A part of the prostate glands was immediately frozen in liquid nitrogen and stored at −80°C until processed. Testosterone and estrogen levels in serum were analyzed using radioimmunoassay by a commercial laboratory (SRL, Inc., Tokyo, Japan). The present experiments were performed under protocols approved by the Institutional Animal Care and Use Committee of Nagoya City University Graduate School of Medical Sciences.

Assessment of Prostate Neoplastic Lesion Development

Neoplastic lesions in the prostate gland of TRAP rats were evaluated as previously described [14]. Briefly, neoplastic lesions were classified into three types: low-grade PIN (LG-PIN), high-grade PIN (HG-PIN), and adenocarcinoma. The relative numbers of acini with the histological characteristics of each type, that is, LG-PIN, HG-PIN, and adenocarcinoma, were quantified by counting the total acini in each prostatic lobe.

Immunoblot Analysis

Immunoblot analysis was performed as described previously [15]. Briefly, frozen ventral prostate tissues were homogenized in RIPA buffer (150 mM NaCl, 50 mM Tris–HCl (pH 8.0), 1% NP-40, 0.5% sodium deoxycholate, 0.1% SDS, 1 mM phenylmethylsulphonyl fluoride, 1 mM sodium orthovanadate, and protease inhibitor cocktail [Complete, Roche]). The antibodies used were cyclin D1 (Oncogene Science, Cambridge, MA), caspases 3, 7, and 9, Erk 1/2 and phophs-Erk1/2, p38 MAPK and phospho-p38 MAPK (Cell Signaling Technology, Danvers, MA), AR and SV40 T antigen (Santa Cruz Biotechnology, Inc., Santa Cruz, CA), VEGF (IBL Co. Ltd., Fujioka, Japan) and β-actin (Sigma). The intensity of each band was measured using Image J 1.440 (National Cancer Institute, Bethesda, MD).

Immunohistochemistry

Deparaffinized sections were incubated with diluted antibodies for Ki-67 (Novocastra Laboratories Ltd., Newcastle, UK), SV40 T antigen (Santa Cruz Biotechnologies), phospho-p38 MAPK (Thr180/Tyr182), and cleaved caspase 3 (Asp175: Cell Signaling Technology, Danvers, MA). Apoptotic cells in the prostate were detected using an In Situ Apoptosis Detection Kit (TUNEL method) according to the manufacturer's instructions (Takara Bio Inc., Ohtsu, Japan). Labeling indices for Ki-67, TUNEL, cleaved caspase 3 or phospho-p38 MAPK were generated by counting over 1,000 cells mainly in HG-PIN under microscope at high magnification and they were expressed as numbers of positive cells per 100 cells. To evaluate the effect of telmisartan against angiogenesis, microvessels were detected using anti-factor 8-related antigen (DAKO, Glostrup, Denmark).

Cell Proliferation Assay

Cell proliferation of prostate cancer cell lines was assessed by 4-[3-(4-iodophenyl)-2-(4-nitrophenyl)-2H-5-tetrazolio]-1,3-benzene disulfonate tetrazolium salt (WST-1) assay (Roche Applied Science, Mannheim, Germany). Briefly, cells were seeded in 96-well plates at 1×10^4 cells/well in 200 μl of culture media. ARBs or ERβ agonists were added 24 hrs after seeding and incubated for 3 days. WST-1 reagent was added to each well with incubation for 60 min at 37°C, and then each well were measured for absorbance at 430 nm.

Ubiquitylation Assay

LNCaP cells were transfected with Flag-tagged human AR (pCMVTag/hAR) using Nucleofector II (Amaxa AG, Koeln, Germany), seeded into a 6-well plate and incubated for 24 hr. Cells were treated with ARBs and/or 1 μM MG132 for 24 hr, and then lysed with RIPA buffer supplemented with COMPLETE protease inhibitor cocktail (Roche Diagnostics GmbH, Mannheim, Germany). The extracts were immunoprecipitated with anti-Flag antibody (Sigma) and protein G sepharose (GE Healthcare Bio-sciences AB, Uppsala, Sweden) for 3 hr at 4°C. After washing the agarose with RIPA buffer, Laemmli sample buffer was directly added to the agarose and heated to 85°C for 10 min. Samples were subjected to immunoblot analysis using anti-ubiquitin antibody (Santa Cruz).

Reporter Gene Assay

LNCaP cells were transfected with the pGL3/PSA promoter using Nucleofector II. Twenty-four hours after transfection, 5 nM DHT and/or ARB was added.

Cells were lysed with the buffer supplied in the kit 72 hr after transfection. The luciferase assay was conducted using the dual-luciferase reporter assay system (Promega Corporation, Madison, WI) according to manufacturer's protocol. Data shown represent the mean and standard deviation of four independent data points.

Microarray Analysis

Total RNA was isolated from ventral prostate tissues as en bloc by phenol–chloroform extraction (ISOGEN, Nippon Gene Co. Ltd., Toyama, Japan), and fluorescent cRNA amplification was performed using a Low RNA Input Fluorescent Linear Amplification kit (Agilent Technologies, Palo Alto, CA) according to the manufacturer's instruction. Total RNA from ventral prostate of F344 rat was used as a reference RNA. Quality of total and amplified cRNAs was examined with a high-resolution electrophoresis system, Agilent 2100 Bioanalyzer (Agilent Technologies). Gene expression analysis was performed using a Whole Rat Genome oligo DNA microarray (4 × 44k; Agilent Technologies). The slides were hybridized with Cy3- or Cy5-labeled cRNA for 16–18 hr at 60°C, washed in 0.5 × SSC/0.01% SDS buffer for 5 min at room temperature, then 0.06 × SSC buffer for 2 min, and desiccated with a centrifuge. The slides were scanned with a DNA Microarray Scanner (Agilent Technologies) at two wavelengths to detect emission from both Cy3 and Cy5. Genes with significantly different expression levels were revealed by Significance Analysis of Microarray (ver 2.0; delta = 0.34; http://www-stat.stanford.edu/~tibs/SAM/).

Real-Time RT-PCR

Total RNA was isolated from ventral prostate tissues as en bloc using an RNeasy Mini kit (Qiagen, Valencia, CA). Total RNAs were reverse-transcribed with the Thermoscript first-strand synthesis system (Invitrogen Corporation, Carlsbad, CA), and real-time RT-PCR was performed using a LightCycler (Roche Diagnostics GmbH). The oligonucleotides listed in Table S1 as primers.

RNA-Interference

siRNAs were designed and obtained from RNAi Co. Ltd. (Tokyo, Japan), AR, ERβ and control siRNA sequences were 5′-GAGGAGCUUUCCAGAAUCUGU-3′, 5′-GGAAAUGCGUAGAAGGAAUUC-3′ and 5′-GUACCGCACGUCAUUCGUAUC-3′, respectively. LNCaP cells were transfected with siRNAs using Nucleofector II.

Statistical Analysis

Differences in incidences or means between groups were determined by analysis of variance (ANOVA), followed by the Dunn' multiple comparison test or Dunnett's post-hoc test with GraphPad Prism (version 5.0c; GraphPad Software, Inc., La Jolla, CA), respectively.

Intervention Study

After Institutional Review Board approval was obtained, data from 234 patients undergoing radical prostatectomy (RP) at Yokohama City University Hospital and Center Hospital from March 1999 to July 2007 were entered into our database. Biochemical failure (BCF) was defined as a single PSA level of □ 0.2 ng/ml. The PSA-doubling time (DT) was calculated by log-linear regression and analyzed, respectively, as from the nadir PSA level after RP up to 0.2 ng/ml, and from 0.2 ng/ml to about 1.0 ng/ml. Briefly, PSA-DT was calculated starting with the nadir PSA value after RP, and included all PSA values up to 0.2 ng/ml used in the PSA-DT calculations, and also required patients to have a minimum of two values separated by at least 3 months, which was designated as ePSA-DT. In cases with a PSA value over 0.2 ng/ml, PSA-DT was calculated using PSA values after BCF (i.e., □ 0.2 ng/ml), as opposed to ePSA-DT, which was computed using all values after BCF up to about 1.0 ng/ml, at which point secondary therapy, for example, radiotherapy or hormonal therapy, was started, which was designated as aPSA-DT.

Eighteen patients were enrolled in this study. All patients underwent RP, and the specimens showed adenocarcinoma pathologically, with tumor stage T2 or T3, without lymph node metastasis (pathological stage: T2 or T3 N0M0). At BCF of PSA values, they received olmesartan (Dai-ichi Sankyo Co., Tokyo, Japan), an ARB, at 10–20 mg once daily till they received secondary therapy when their PSA values were over 1.0 ng/ml. ePSA-DT was calculated using all PSA values from the PSA nadir after RP until the start of olmesartan. Then, aPSA-DT was calculated using all PSA values after the start of olmesartan to the start of secondary therapy, at which point their PSA values were over 1.0 ng/ml. As for the control, 9 patients were not treated after RP until PSA level was over 1.0 ng/ml. ePSA-DT was calculated starting with the nadir PSA value after RP and included all PSA values up to 0.2 ng/ml, and aPSA-DT was calculated using all PSA values from BCF (□ 0.2 ng/ml) to over 1.0 ng/ml.

We compared ePSA-DT and aPSA-DT of olmesartan-treated patients and control patients. Also, the ratio of aPSA-DT/ePSA-DT was compared between

olmesartan-treated patients and control patients by Wilcoxon signed-rank test. Furthermore, the time to PSA progression over 1.0 ng/ml after BCF and from the nadir PSA value ($TTPP_{1.0}$) was estimated using Kaplan–Meier method and analyzed using log rank test.

RESULTS

Animal Experiment UsingTRAP Rats

Experiment 1. One rat in the control group was omitted from the effective animals because of suffering from cachexia due to the spontaneous development of leukemia. Blood pressure of TRAP rats treated with telmisartan was significantly lowered in a dose-dependent manner (Table S2). Telmisartan decreased mean body weight and increased kidney weight but did not influence the ventral prostate and liver weights (Table S2, Fig. S2A). Histologically, stromal edema was demonstrated in the kidneys of TRAP rats given telmisartan but tubular or glomerular damage was not evident (Fig. S2C). Serum levels of testosterone and estradiol were not affected by telmisartan (Table S2). In the lateral prostate, a significant decrease in the incidence of adenocarcinoma was observed (Table I). In the ventral prostate, there was a marked or partial pathologic response to telmisartan treatment, as demonstrated by a significant reduction in the amount of prostatic neoplastic lesions in TRAP rats; however, small foci of adenocarcinoma still remained, so there was no significant difference in the incidence of PIN or adenocarcinoma in the prostate of TRAP rats (Table I). Quantitative evaluation of the proportion of preneoplastic and neoplastic lesions in the prostate gland showed significant suppression of progression from LG-PIN to HG-PIN or adenocarcinoma in rats treated with telmisartan (Table II). There was a significant increase in the apoptotic index in the prostate of TRAP rats given telmisartan (Fig. 1A), although Ki-67 index was not different among the groups (Fig. 1B). In the ventral prostate, immunoblot analyses showed activation of caspases 3 and 7 and inactivation of p38 MAPK in rats treated with telmisartan, while expression of cyclin D1 was not altered in all groups (Fig. 1E). Both caspase 3 activation and decreased expression of phospho-p38 MAPK were confirmed by immunohistochemistry (Fig. 1G,I). There was no difference in the expression of AT1R in the ventral prostate between telmisartan-treated and control rats (Fig. 1K). ARB exerted suppressive effects on the growth of prostate cancer via the inhibition of angiogenesis in a tumor xenograft model [16]. The possibility that telmisartan augmented apoptosis in prostate cancer through suppression of tumor angiogenesis in TRAP rats was examined. Unexpectedly, VEGF protein expression in the ventral prostate was not altered by telmisartan treatment (Fig. S3), and there was no difference in microvessel density among the groups (Table S3).

Experiment 2. To confirm the reproducibility of the suppressive effect of telmisartan on prostate carcinogenesis, we performed an experiment with a similar design to that of experiment 1. Candesartan, a selective AT1R blocker with no PPARγ agonistic activity at usual doses, was applied for comparison with the effects of telmisartan. Body weight gain and organ weights were not affected by candesartan (Table S4, Fig. S2B). Serum levels of testosterone and estradiol were not significantly different between telmisartan and candesartan treatment (Table S4). Prostate adenocarcinomas were found only in the ventral and lateral lobes, and a significant decrease in its incidence was observed in the lateral prostate and suppression of the progression of prostatic lesions from LG-PIN to

TABLE I. Incidences of Adenocarcinoma of the Prostate Glands of TRAP Rats

Treatment	No. of rats	Ventral AC (%)	Lateral AC (%)	Dorsal AC (%)
Experiment 1				
Control	11	11 (100)	9 (82)	0
TS 2 mg/kg/day	12	11 (92)	8 (67)	0
TS 10 mg/kg/day	12	9(75)	4 (33)*	0
Experiment 2				
Control	12	12(100)	12 (100)	0
CS 2 mg/kg/day	12	12(100)	10 (83)	0
CS 10 mg/kg/day	12	11 (92)	5 (42)**	0
TS 10 mg/kg/day	12	12(100)	4 (33)**	0

TS, telmisartan; CS, candesartan; AC, adenocarcinoma.
*P □ 0.05 versus control.
**P □ 0.01 versus control.